DEVELOPMENTS IN BLACK HOLE INFORMATION LOSS PARADOX IN FLAT AND ADS SPACETIME

M.Sc. Thesis

By VARUN VIJAY BHALERAO





INDIAN INSTITUTE OF TECHNOLOGY INDORE

CANDIDATE'S DECLARATION

I hereby certify that the work which is being presented in the thesis entitled Developments in Black Hole information loss paradox in flat and AdS spaces in the partial fulfillment of the requirements for the award of the degree of MASTER OF SCIENCE and submitted in the DISCIPLINE OF PHYSICS, Indian Institute of Technology Indore, is an authentic record of my own work carried out during the time period from July 2023 to February 2025 under the supervision of Dr. Mritunjay Kumar Verma, (Assistant Professor) Department of Physics, IIT Indore.

The matter presented in this thesis has not been submitted by me for the award of any other degree of this or any other institute.

Signature of the student with date (VARUN VIJAY BHALERAO)

This is to certify that the above statement made by the candidate is correct to the best of my knowledge.

writingy Kuma

Signature of the Supervisor of

(Dr. Mritunjay Kumar Verma)

Varun Vijay Bhalerao has successfully given his M.Sc. Oral Examination held on $13 \, Mav \, 2025$.

Signature of Supervisor of MSc thesis

Nitingy Kumy

Date: **18 May 2025**

Convener, DPGC

Date: 20-05-25

ACKNOWLEDGEMENTS

This research project has been a very special journey for me. When I started, I didn't have a lab to work in and had very little experience in research. Still, with the constant support, guidance, and belief of so many people around me, I was able to complete this work. I would like to take a moment to thank everyone who helped me in one way or another along the way.

First of all, I am truly grateful to my project supervisor, Dr. Mritunjay Kumar Verma, for his constant guidance, patience, and support. He always encouraged me to ask questions, think deeply, and keep learning. His calm and understanding nature made it easy for me to approach him, and I learned so much under his mentorship—not just about the subject, but also about how to stay focused and curious.

I would also like to give special thanks to the Learning Resource Centre (LRC). Since I didn't have access to a lab, the library became my main place to work. It gave me a quiet space and all the resources I needed to do my research. I spent countless hours there, and it truly became an important part of my journey.

To my friends Deepam Sharma, Lakhyanath Kuli, and Suman Birda—thank you for always being there for me and keeping me motivated. Your support meant a lot. A big thank you to my best friend, Vaibhav Yenare, who stood by me through every challenge—both in academics and in life. His help and belief in me gave me strength during the toughest moments.

I would also like to thank my senior who supported me quietly during difficult times. Her kindness and understanding helped me get through many emotionally challenging moments, and I will always appreciate her presence during those times.

Most importantly, I want to thank my parents, Didi, and Aai. Their love, support, and belief in me have been the biggest reason I could keep going. They were always there in my highs and lows, and their presence gave me the confidence to push through even the hard days. I will always be grateful for everything they have done for me.

In the end, this journey was full of learning, growth, and support from people who truly cared. To everyone who helped me, directly or indirectly—thank you from the bottom of my heart.

DEDICATION

In loving memory of Jackson and Muffy

ABSTRACT

This project was aimed to understand the Black Holes information loss paradox. Classical general relativity demands that nothing can escape from the black hole. However, quantum mechanics shows that particles can emit from the black hole with a thermal spectrum. In this project, several developments were carried out to understand this paradox.

List of Figures

3.1 3.2	World lines with $R = const$ indicate particles at fixed radial positions Kruskal coordinate representation of a spherically symmetric vac-	5 7
	uum spacetime	·
4.1	IN-, UP-, OUT- and DOWN-modes	11
5.1	Conformal (Penrose-Carter) diagram of a Schwarzschild black hole formed via the spherical collapse of a thin null shell	14
8.1	A Penrose diagram describing the collapse of a star to form a black hole	24
8.2	Outgoing null geodesics from a Cauchy hypersurface leading to a distant observer	25
9.1	Derivation of the Hawking process using a late-time Cauchy hypersurface	34
10.2	A Schematic representation of the Rindler Wedges and causal regions Euclidean path integrals for vacuum and density matrices	41

Contents

1	INTRODUCTION	1
2	Brief History of Blackhole 2.0.1 What is a Blackhole?	2
3	Spherically Symmetric Black Holes 3.1. Schwarzschild Metric	
4	Black hole Perturbations 4.1. Perturbative Behavior in Schwarzschild Background 4.1.1 Dynamics of scalar fields around a spherically symmetric black hole	8
5	•	13 13 13
6	Black Hole Thermodynamics	21
7	Black Hole Entropy And The Generalized Second Law	2 2
8	Black Hole Evaporation	2 4
9	Gray Body Factors 9.1. The Potential Barrier 9.2. More Detailed Argument 9.3. Thermodynamic Instability	31 33 36
10	Thermodynamics of Rindler Space 10.1. Making The Cut	39 39 43 45

Double	48
11 Conclusions and Scope for Future Work	52
Appendices	53
A Regge-Wheeler equation	54
B Deriving equation (3.1)	55
C Deriving equation (3.2)	57
D Deriving equation (3.5)	5 8
E To show equation (3.5) is Antiperiodic in imaginary time:	60
F Wronskian of λ_{ω} and $\tilde{\lambda}_{\omega}$	62

INTRODUCTION

One of the most profound puzzles in contemporary theoretical physics is the information loss paradox associated with black holes. While quantum mechanics explains the strong, weak, and electromagnetic forces, except for gravity, with no experimentally verified quantum theory yet. However, a semi-classical approach lets us combine quantum mechanics with Einstein's general relativity, leading to fascinating insights like **Hawking radiation**— the idea that black holes aren't completely black but emit thermal spectrum of particles.

The information loss paradox arises from Hawking radiation which mainly focuses on fundamental principles of quantum mechanics. As per Quantum theory, information about a system's state cannot be destroyed (a principle called unitarity). However, Hawking radiation appears to carry no information about the matter that fell into the black hole. If the black hole eventually evaporates completely, it raises the important question: What happens to the information about the particles and objects that fell into the black hole? This leads to the paradox because quantum mechanics insists that information must be preserved, but classical general relativity (through black hole evaporation) gives different results. Thus, violating the laws of quantum theory.

The aim of the project is to study the recent developments in resolving the black hole information loss paradox and comparing different approaches in flat and AdS(Anti-de Sitter) spacetimes. The project report is organized as follows: Chapter 2 provides a brief historical overview of black holes. Chapter 3 presents a detailed study of spherically symmetric black holes. Chapter 4 focuses on investigations into black hole perturbations. Chapter 5 examines quantum particle creation by black holes, with an emphasis on modes and bases that are essential steps toward deriving Hawking radiation. Chapter 6 gives introduces Black Hole Thermodynamics. Chapter 7 of this report explores Bekenstein's intuitive argument for black hole entropy. Meanwhile, Chapter 8 and 9 focus on Hawking's groundbreaking discovery of quantum radiation emitted by black holes and how the potential barrier outside the black hole alters Hawking radiation. The last chapter 10 is devoted to Rindler space and the Unruh effect, which provide a simplified framework for understanding some essential aspects of quantum black holes.

Brief History of Blackhole

2.0.1 What is a Blackhole?

- A black hole is defined as a region of spacetime in which the gravitational field becomes so intense that the escape velocity exceeds the speed of light, thereby preventing any form of matter or electromagnetic radiation from escaping beyond its event horizon.
- ullet A black hole is created when an object of mass M undergoes gravitational collapse to a size smaller than its Schwarzschild radius, the critical radius beyond which escape is no longer possible

$$r_g = \frac{2GM}{c^2}$$

- $\bullet \ r_g$ is the Gravitational Radius/Schwarzschild Radius.
- In 1916, Schwarzschild presented the first exact solution to Einstein's vacuum field equations assuming spherical symmetry. This solution contains a singularity at the center (r=0) and another apparent singularity at the gravitational radius $r=r_g$, known as the Schwarzschild radius.

2.0.2 "A Black Hole radiates like a heated Black Body" explain?

- In 1975, Hawking obtained a new unexpected result that changed our understanding on the behavior of the Black Holes, he discovered:

 Vacuum fluctuations in a black hole's strong gravitational field lead to the emission of quantum radiation, commonly referred to as Hawking radiation.
- One of the most notable features of this radiation is its thermal spectrum. In simpler terms, when the influence of external gravitational scattering is ignored, a black hole emits radiation similar to that of a hot black body.

Spherically Symmetric Black Holes

3.1 Schwarzschild Metric

In the presence of a spherically symmetric vacuum spacetime, the solution to Einstein's equations takes the form –

$$ds^{2} = -\left(1 - \frac{2GM}{c^{2}r}\right)c^{2}dt^{2} + \left(\frac{1}{1 - \frac{2GM}{c^{2}r}}\right)dr^{2} + r^{2}(d\theta^{2} + \sin^{2}\theta d\phi^{2})$$
(3.1)

$$ds^{2} = -\left(1 - \frac{R_{g}}{r}\right)c^{2}dt^{2} + \left(\frac{1}{1 - \frac{R_{g}}{r}}\right)dr^{2} + r^{2}(d\theta^{2} + \sin^{2}\theta d\phi^{2})$$
(3.2)

Equation (3.2) is called **Schwarzschild Metric**

$$R_g = \frac{2GM}{c^2}$$
: Schwarzschild Radius

In this equation, G stands for the universal gravitational constant, and M is the mass responsible for the gravitational field. An important property of the Schwarzschild metric is its invariance under time translations in the coordinate t. This metric is fully characterized by one parameter, M, which indicates the entire mass of the object generating the gravitational field.

3.2 Spacetime Within the Schwarzschild Sphere

3.2.1 R- and T-regions

R - region (Radial Region)

The R-region represents the part of spacetime where the radial coordinate r behaves like a spatial coordinate. outside the event horizon of a black hole where $r > r_g$ the radial coordinate r measures the distance from the black hole center. In this region, r increases as you move away from the black hole and t (time) behaves normally; allowing us to move forward in time.

T - region (Temporal Region)

The T-region represents the part of spacetime where the radial coordinate r behaves more like a time coordinate rather than a spatial one. Inside the event horizon, the role of time and space switch in a way. the radial coordinate r starts to act like a time coordinate because all paths (regardless of direction) lead inevitably to smaller r values, ultimately ending at the singularity. In this region, no matter how you move, you are compelled to more towards the singularity at r = 0. the time coordinate t behaves like a spatial coordinate in a certain sense, but with significant difference due to curvature of time.

Key Points:

- Outside the Event Horizon (R-region) Time behaves normally and space behaves as expected.
- Inside the Event Horizon (T-region) The concept of moving through space changes dramatically, with all paths leading towards the singularity and r acting more like a time coordinate.

3.2.2 Advanced null coordinates (Eddington–Finkelstein form)

We examine an alternative coordinate system introduced by Eddington and Finkelstein, which remains regular at the Schwarzschild radius r_g . This frame is adapted to the motion of photons traveling radially. In region $r > r_g$ the photons moving towards the center are characterized by r decreasing with t. equation for such photons can be rewritten in the form -

$$ct = v - r_*$$
, $r_* = r + r_g \ln \left| \frac{r}{r_g} - 1 \right| + \frac{v}{c}$ (3.3)

In this context, r_* is referred to as the tortoise coordinate, and v represents a constant specifying the radial position of a photon at a particular time t. The definition of r_* includes a logarithmic term with the absolute value of r/r_g-1 , ensuring that r_* remains well-defined for both $r>r_g$ and $r< r_g$.

Consider a collection of photons at a fixed coordinate time t, where each photon is labeled by a constant value v that remains invariant along its trajectory. This quantity v, known as advanced time, can be introduced as a new coordinate. It is a null coordinate, meaning it is neither spatial nor temporal in the conventional sense. As the second coordinate, we retain the standard radial coordinate r. By differentiating equation (3.3) and replacing dt with the resulting expression in the metric applicable to regions far from intense gravitational fields, we obtain

$$ds^{2} = -\left(1 - \frac{r_{g}}{r}\right)dv^{2} + 2dvdr + r^{2}(d\theta^{2} + \sin^{2}\theta d\phi^{2})$$
 (3.4)

At $r = r_g$, Equation (3.4) remains regular. At this stage, the coefficient associated with dv^2 reaches zero. The existence of the cross term 2dvdr prevents the metric—and therefore the coordinate system—from becoming degenerate.

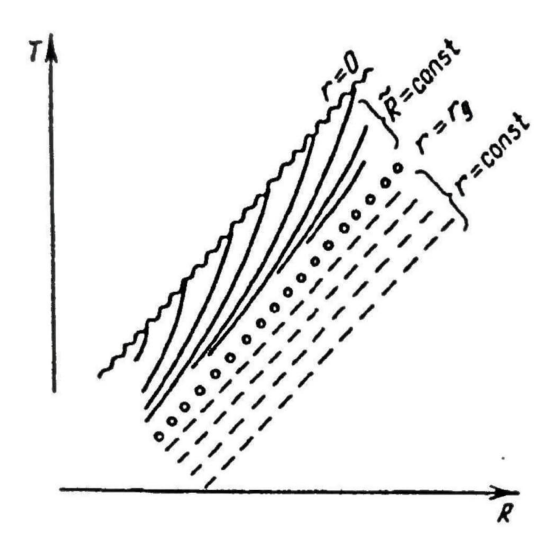


Figure 3.1: The worldlines defined by $\hat{R} = const$ represent the trajectories of particles that establish the reference frame described by Equation (3.37) in Lemaître coordinates

A non-degenerate metric ensures that our space has a constant and meaningful way of measuring distances and angles. if a metric become degenerate, we'll lose the ability to make these measurements correctly, leading to breakdown in our understanding of the geometry of the space.

We now adopt an alternative form of Eddington-Finkelstein coordinates (u, r, θ, ϕ) , where $u = ct - r_*$ denotes the **retarded time**. In these coordinates, the Schwarzschild metric becomes:

$$ds^{2} = -\left(1 - \frac{r_{g}}{r}\right)du^{2} - 2dudr + r^{2}(d\theta^{2} + \sin^{2}\theta d\phi^{2})$$
 (3.5)

3.2.3 Kruskal coordinates

Kruskal coordinates provide a complete description of the spacetime encompassing both eternal black holes and white holes. Within this framework, the metric is represented in the form -

$$ds^{2} = \frac{4r_{g}^{3}}{r} e^{-(r/r_{g}-1)} \left(-d\tilde{T}^{2} + d\tilde{R}^{2} \right) + r^{2} (d\theta^{2} + \sin^{2}\theta d\phi^{2})$$
 (3.6)

Where r is a function of \tilde{T} and \tilde{R} -

$$\left(\frac{r}{r_g} - 1\right) e^{-(r/r_g - 1)} = \tilde{R}^2 - \tilde{T}^2$$
 (3.7)

The regions R' and R'' are defined in these coordinates by $\tilde{R} > |\tilde{T}|$ and $(-\tilde{R} > |\tilde{T}|)$, respectively. Similarly, the regions T_- and T_+ satisfy $\tilde{T} > |\tilde{R}|$ and

 $(-\tilde{T}>|R|)$, respectively. The curvature singularity at r=0 is represented by the curve $\tilde{T}^2-\tilde{R}^2=e^{-1}$.

In regions R' and T_- , the coordinates (\tilde{T}, \tilde{R}) are related to (r, t) through the following equations:

$$In R'(for r > r_g) : \begin{cases} \tilde{R} = (r/r_g - 1)^{1/2} e^{(r-r_g)/2r_g} \cosh(ct/2r_g), \\ \tilde{T} = (r/r_g - 1)^{1/2} e^{(r-r_g)/2r_g} \sinh(ct/2r_g), \end{cases}$$
(3.8)

$$In T_{-}(for \ r < r_g) : \begin{cases} \tilde{R} = (1 - r/r_g)^{1/2} e^{(r-r_g)/2r_g} \sinh(ct/2r_g), \\ \tilde{T} = (1 - r/r_g)^{1/2} e^{(r-r_g)/2r_g} \cosh(ct/2r_g), \end{cases}$$
(3.9)

Similar expressions for the R'' and T_+ regions can be obtained by substituting $\tilde{R} \to -\tilde{R}$ and $\tilde{T} \to -\tilde{T}$.

$$In R''(for r > r_g) : \begin{cases} -\tilde{R} = (r/r_g - 1)^{1/2} e^{(r-r_g)/2r_g} \cosh(ct/2r_g), \\ -\tilde{T} = (r/r_g - 1)^{1/2} e^{(r-r_g)/2r_g} \sinh(ct/2r_g), \end{cases}$$
(3.10)

$$In T_{+}(for \ r < r_g) : \begin{cases} -\tilde{R} = (1 - r/r_g)^{1/2} e^{(r-r_g)/2r_g} \sinh(ct/2r_g), \\ -\tilde{T} = (1 - r/r_g)^{1/2} e^{(r-r_g)/2r_g} \cosh(ct/2r_g), \end{cases}$$
(3.11)

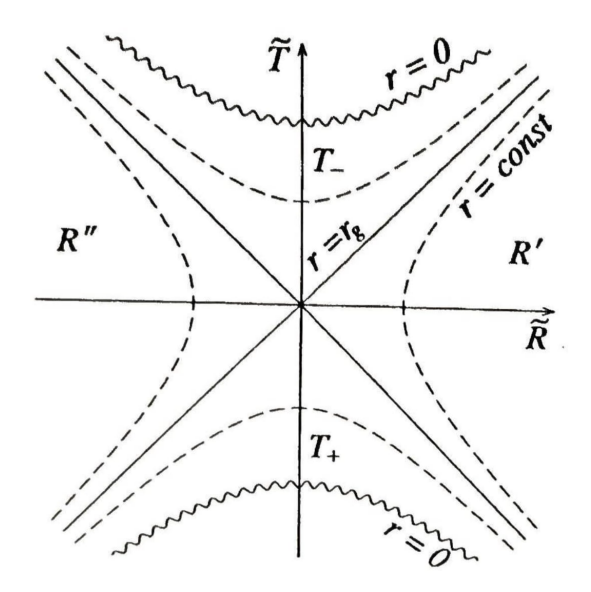


Figure 3.2: Representation of Spherical Vacuum Spacetime Using Kruskal Coordinates.

The advantage of using Kruskal coordinates is that radial null geodesics appear as straight lines angled at 45° relative to the coordinate axes. It is common to use null coordinates $U = \tilde{T} - \tilde{R}$ and $U = \tilde{T} + \tilde{R}$ in place of (\tilde{R}, \tilde{T}) . In terms of these coordinates, the Kruskal metric is expressed as:

$$ds^{2} = \frac{4r_{g}^{3}}{r} e^{-(r/r_{g}-1)} dV dU + r^{2} (d\theta^{2} + \sin^{2}\theta d\phi^{2})$$
 (3.12)

$$-UV = \left(\frac{r}{r_g} - 1\right) \exp\left(\frac{r}{r_g} - 1\right) \tag{3.13}$$

Within Kruskal coordinates, the condition $r = r_g$ aligns with either U = 0 or V = 0. The boundary U = 0, defines the **event horizon**, separating the exterior region R' from the black hole region T_- . Similarly, V = 0 marks the **past horizon**, dividing the exterior from the white hole region.

Black hole Perturbations

4.1 Perturbative Behavior in Schwarzschild Background

4.1.1 Dynamics of scalar fields around a spherically symmetric black hole.

A massless scalar field Φ evolves according to the Klein-Gordon equation :

$$\Box \Phi \equiv (-g)^{-1/2} \, \partial_{\mu} \left[(-g)^{1/2} \, g^{\mu\nu} \, \partial_{\mu} \Phi) \right] = 0 \tag{4.1}$$

where g is the determinant of the metric tensor $g_{\mu\nu}$. The Schwarzschild metric is given by :

$$ds^{2} = -\left(1 - \frac{2M}{r}\right)dt^{2} + \left(\frac{1}{1 - \frac{2M}{r}}\right)dr^{2} + r^{2}(d\theta^{2} + \sin^{2}\theta d\phi^{2})$$
(4.2)

As the metric exhibits spherical symmetry, we can apply the following mode decomposition:

$$\Phi_{\ell m} = \frac{u_{\ell}(r,t)}{r} Y_{\ell m}(\theta,\phi]) \tag{4.3}$$

Here, $\frac{u_l(r,t)}{r}$ represents the Radial term and $Y_{lm}(\theta,\phi]$ represents the Angular term. Substituting (4.3) in (4.1) yields:

$$\left[\frac{\partial^2}{\partial r_*^2} - \frac{\partial^2}{\partial t^2} - V_\ell(r)\right] u_\ell(r, t) = 0$$
(4.4)

The equation above makes use of the tortoise coordinate r_* , previously defined in the last chapter, which corresponds with the usual Schwarzschild radius r through the equation:

$$\frac{d}{dr_*} = \left(1 - \frac{2M}{r}\right) \frac{d}{dr} \tag{4.5}$$

or

$$r_* = r + 2M \log\left(\frac{r}{2M} - 1\right) + constant. \tag{4.6}$$

With the additional assumption of harmonic time dependence, where $u_{\ell}(r,t) = \hat{u}_{\ell}(r,\omega) e^{-i\omega t}$, we arrive at the following ODE:

$$\left[\frac{\partial^2}{\partial r_*^2} - \frac{\partial^2}{\partial t^2} - V_\ell(r)\right] \hat{u}_\ell(r,\omega) e^{-i\omega t} = 0$$
(4.7)

If we further simplify (4.7) we'll get the following equation (see Appendix A)

$$\left[\frac{\partial^2}{\partial r_*^2} + \omega^2 - V_\ell(r)\right] \hat{u}_\ell(r,\omega) = 0 \tag{4.8}$$

Equation (4.8) is known as the **Regge-Wheeler equation**, and its associated effective potential is expressed as follows:

$$V_{\ell}(r) = \left(1 - \frac{2M}{r}\right) \left[\frac{\ell(\ell+1)}{r^2} + \frac{2M}{r^3} \right]$$
 (4.9)

Here, M denotes Black hole's mass. The study of perturbed black holes often draws upon principles commonly encountered in quantum mechanical potential scattering. Waves with very short wavelengths, where $\lambda \ll 2M$, can pass through the barrier with little resistance. Waves with wavelengths on the order of $\lambda \sim 2M$ undergo partial transmission and partial reflection. In contrast, waves of much longer wavelengths, $\lambda \gg 2M$, are expected to be argely reflected due to the black hole's potential barrier.

Since, the potential approaches zero both at infinity and at the horizon, the two independent solutions of equation (4.8) asymptotically behave as follows:

$$\hat{u}_{\ell}(r,\omega) \sim e^{\pm i\omega r_*} \tag{4.10}$$

As $r \to +\infty$ and $r \to 2M$. The tortoise coordinate deviates from a standard radial coordinate due to the presence of a logarithmic term. Consequently, r_* tends to $+\infty$ at spatial infinity $(r \to +\infty)$, While it approaches $-\infty$ near the event horizon $(r \to 2M)$.

4.1.2 A fundamental set of solutions serving as a basis for further analytical development

To simplify the analysis of wave equations in black hole spacetimes, one can use an eternal black hole with the same parameters as the late-time spacetime. This allows well-defined solutions to be constructed by setting boundary conditions at past infinity and the past event horizon. Based on the asymptotic form given in equation (4.10), it becomes straightforward to identify solutions to equation (4.8) that meet these boundary requirements. A particularly natural choice involves enforcing the physical condition that **no waves originate from the black hole**. we call this solution as **IN-mode Solution**, which is defined by:

$$\hat{u_{\ell}}^{in}(r_*, \omega) \sim \begin{cases} e^{-i\omega r_*}, & r_* \to -\infty, \\ A_{out}(\omega) e^{i\omega r_*} + A_{in}(\omega) e^{-i\omega r_*}, & r_* \to +\infty, \end{cases}$$
(4.11)

The complex conjugate of IN-mode Solution is the **OUT-mode Solution** and it is defined as:

$$\hat{u_{\ell}}^{out}(r_*, \omega) \sim \begin{cases} e^{i\omega r_*}, & r_* \to -\infty, \\ A_{out}(\omega) e^{-i\omega r_*} + A_{in}(\omega) e^{i\omega r_*}, & r_* \to +\infty, \end{cases}$$
(4.12)

Now, Since the Wronskian of any pair of linearly independent solutions to equation (4.8) is constant, it is appropriate to consider $\hat{u_\ell}^{in}$ along with its complex conjugate $\hat{u_\ell}^{out}$ and evaluating Wronskian at $r_* = \pm \infty$, one can show that:

• At $r_* = -\infty$:

$$\hat{u_{\ell}}^{in} \sim e^{-i\omega r_*}$$
 ; $\hat{u_{\ell}}^{out} \sim e^{i\omega r_*}$
$$W\left[\hat{u_{\ell}}^{in}, \hat{u_{\ell}}^{out}\right] = 2i\omega$$
 (4.13)

• At $r_* = +\infty$:

$$\hat{u_{\ell}}^{in} \sim A_{out}(\omega) e^{i\omega r_*} + A_{in}(\omega) e^{-i\omega r_*}$$

$$\hat{u_\ell}^{out} \sim A_{out}(\omega) e^{-i\omega r_*} + A_{in}(\omega) e^{+i\omega r_*}$$

$$W\left[\hat{u_{\ell}}^{in}, \hat{u_{\ell}}^{out}\right] = 2i\omega \left(|A_{in}|^2 - |A_{out}|^2\right)$$

$$(4.14)$$

Since, Wronskian must be constant therefore,

$$2i\omega = 2i\omega \left(|A_{in}|^2 - |A_{out}|^2 \right)$$

$$1 + |A_{out}|^2 = |A_{out}|^2 (4.15)$$

We now define the reflection (R) and transmission (T) amplitudes:

$$T = \frac{1}{A_{in}} \quad , \quad R = \frac{A_{out}}{A_{in}} \tag{4.16}$$

This corresponds to the standard form of a scattering relation.

$$|T|^2 + |R|^2 = 1 (4.17)$$

Consequently, the portion of the incident wave that is not absorbed by the black hole is reflected back toward spatial infinity. The magnitudes |T| and |R| are referred to as the transmission and reflection coefficients (or probabilities), respectively.

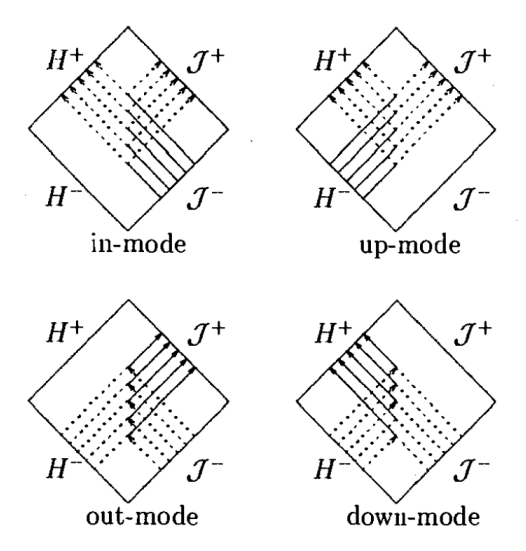


Figure 4.1: IN-, UP-, OUT- and DOWN-modes.

Another fundamental pair of solutions, known as the UP- and DOWN-modes, can be constructed analogously. The **UP-mode** is characterized by **purely outgoing waves at spatial infinity** and is defined as follows:

$$\hat{u_{\ell}}^{up}(r_*, \omega) \sim \begin{cases} B_{out}(\omega) e^{i\omega r_*} + B_{in}(\omega) e^{-i\omega r_*}, & r_* \to -\infty, \\ e^{i\omega r_*}, & r_* \to +\infty, \end{cases}$$
(4.18)

The **DOWN-mode** is the complex conjugate of (4.18) and is defined as:

$$\hat{u_{\ell}}^{down}(r_*, \omega) \sim \begin{cases} B_{out}(\omega) e^{-i\omega r_*} + B_{in}(\omega) e^{i\omega r_*}, & r_* \to -\infty, \\ e^{-i\omega r_*}, & r_* \to +\infty, \end{cases}$$
(4.19)

The coefficients appearing in equation (4.18) are related to those that characterize the IN-mode and are therefore not independent. By employing the constancy of the Wronskian, we obtain the following relation:

$$B_{out}(\omega) = A_{in}(\omega), \tag{4.20}$$

$$B_{in}(\omega) = -\bar{A}_{out}(\omega) = -A_{out}(-\omega). \tag{4.21}$$

The complex conjugate is indicated by an overbar. Any two modes from the set defined above—IN, UP, OUT, and DOWN—may be selected as a basis for solving a given problem. The IN–UP mode combination, together with the Wronskian, will generally be used in the following discussions.

$$W(IN, UP) \equiv \hat{u_{\ell}}^{in} \frac{d\hat{u_{\ell}}^{up}}{dr_{*}} - \hat{u_{\ell}}^{up} \frac{d\hat{u_{\ell}}^{in}}{dr_{*}} = 2i\omega A_{in}(\omega) = 2i\omega B_{out}(\omega)$$
 (4.22)

Let us now consider the physical interpretation of these solutions. By combining the radial solutions with the time-dependent factor $e^{-i\omega t}$, we obtain full waveforms that describe the propagation of waves in the black hole spacetime. These solutions have clear physical meanings. The DOWN-mode is characterized by the boundary condition that no radiation escapes to spatial infinity. This requires that a precisely tuned amount of radiation, with an exact phase, must emerge from the past event horizon (\mathcal{H}^-) to cancel any potential outgoing radiation that would otherwise result from an incoming wave originating at past null infinity (\mathcal{J}^-). Consequently, the DOWN-mode includes three components: radiation arriving from past infinity, radiation emitted from \mathcal{H}^- to interfere with it, and radiation absorbed by the black hole through the future horizon (\mathcal{H}^+) . The amplitudes of these components are such that the DOWN-mode satisfies the radial wave equation (4.7) in a physically consistent manner. Analogously, the UP-mode is defined by imposing the boundary condition that no radiation arrives from spatial infinity. Similarly, the IN-mode excludes any outgoing radiation from \mathcal{H}^- , while the OUT-mode is defined by the absence of radiation falling into the black hole through \mathcal{H}^+ . These scenarios are visually illustrated in Figure 4.1, where the shaded regions represent the exterior spacetime of an eternal black hole. The diagonal lines inclined a 45° indicate null trajectories. The boundaries labeled \mathcal{J}^+ and \mathcal{J}^- represent future and past null infinity, respectively, while H+ and H- correspond to the event horizon and the past horizon.

Quantum Behavior in Black Hole Spacetimes

5.1 Particles from the Void: Black Holes as Quantum Sources

5.1.1 Modes and bases

Model

We initiate our analysis by considering a massless, neutral scalar field φ in the spacetime geometry of an uncharged, non-rotating black hole. We begin by examining a simplified model in which the collapsing object is idealized as a massive, infinitesimally thin shell moving at the speed of light. The spacetime geometry corresponding to this scenario can be expressed through the following metric:

$$ds^{2} = -\left(1 - \frac{2M(v)}{r}\right)dv^{2} + 2dvdr + r^{2}d\omega^{2}$$
(5.1)

Here, $d\omega^2$ denotes the metric on the unit sphere, and the mass function is given by $M(v) = M\vartheta(v - v_o)$. The spacetime is flat for $v < v_o$, corresponding to the region inside the collapsing shell. For $v > v_o$, the geometry transitions to that of the Schwarzschild solution, where M represents the mass of the resulting black hole (refer to Figure 5.1). We now analyze a null ray moving radially that reaches future null infinity, \mathcal{J}^+ , at retarded time u (identified as ray 1 in Figure 5.1). By extending this ray backward in time, we define the advanced time coordinate v = U(u), indicating the point at which the ray originated from past null infinity, \mathcal{J}^- . To fix the origin of the v coordinate, we adopt the convention that the null ray emitted from \mathcal{J}^- at v = 0 arrives at the central point r = 0 precisely at the formation of the event horizon. With this choice of coordinates, it follows directly that the horizon formation occurs at $v_o = 4M$.

Outside the collapsing shell, within the Schwarzschild region, the propagation of an outgoing null ray is governed by the following equation:

$$u = v - 2r_* = const, (5.2)$$

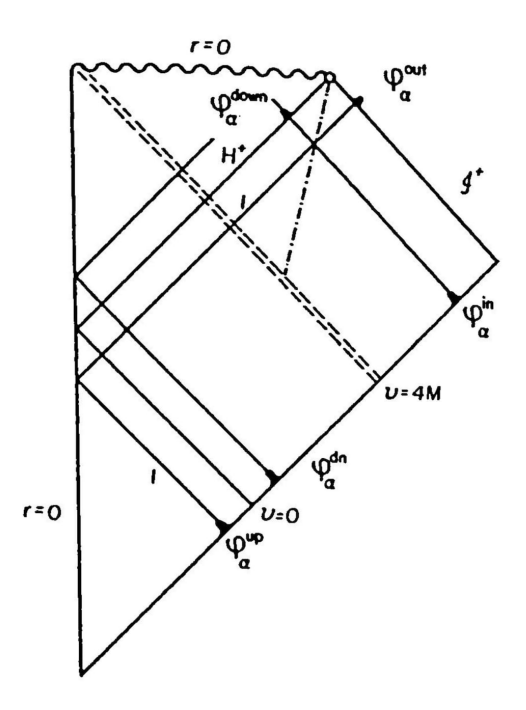


Figure 5.1: Penrose—Carter conformal diagram representing the spacetime of a spherically symmetric, uncharged, and non-rotating black hole formed through the collapse of a spherically symmetric massive null shell.

Here, r_* denotes the tortoise coordinate. The null ray intersects the collapsing shell at v = 4M and at a radial position r = R, where R satisfies the following equation:

$$u = 8M - 2R - 4M \ln[(R - 2M)/2M] \tag{5.3}$$

Null rays that arrive at \mathcal{J}^+ at very late times $(u\to\infty)$ pass through the collapsing shell at a radius approximately equal to 2M, implying that for these late-time rays, we have -

$$u \approx -4M \ln[(R - 2M)/2M] \tag{5.4}$$

Consider an incoming radial null ray emitted from \mathcal{J}^- at a time v < 0. This ray travels through flat spacetime until it intersects the collapsing shell from the inside. For this ray, the coordinate v is constant, given by v = t + r, so it reaches r = 0 at the time t = v. After passing through the origin (r = 0), it continues as an outgoing ray, following the trajectory described by u = t - r = v = const, until it encounters the shell again. The radius R at which the ray intersects the shell is determined by the following relation -

$$v = -2(R - 2M) (5.5)$$

Upon examining equations (5.4) and (5.5), the resulting expression can be written as:

$$u \approx -\kappa^{-1} \ln(-\kappa v) \tag{5.6}$$

This relation connects the advanced time v at which a late-time ray departs from \mathcal{J}^- with the retarded time u at which it arrives at \mathcal{J}^+ . In this context, $\kappa = (4M)^{-1}$ represents the surface gravity of the black hole.

Modes

The dynamics of the massless scalar field φ are governed by the wave equation:

$$\Box \varphi = 0 \tag{5.7}$$

In spherically symmetric spacetime, the solutions can be represented through a mode decomposition

$$\varphi_{\ell m} = \frac{u_{\ell}(r,t)}{r} Y_{\ell m}(\theta,\phi])$$
(5.8)

Our objective now is to establish appropriate sets of mode solutions that will enable the definition of convenient in- and out-bases for the quantum field $\hat{\varphi}$. One specific type of solution, called outgoing modes $\varphi_{\ell m \omega}^{out}(x)$, is defined with the with the condition that they vanish on the black hole's event horizon (H^+) and exhibit the following asymptotic form near \mathcal{J}^+ .

$$\varphi_{\ell m \omega}^{out} \sim \frac{1}{r} \Phi_{\ell m \omega}^{out} = \frac{1}{\sqrt{4\pi\omega}} \frac{e^{-i\omega u}}{r} Y_{\ell m}(\theta, \phi)$$
 (5.9)

We refer to $\Phi_{\ell m \omega}^{out}$ as the projection of the field $\varphi_{\ell m \omega}^{out}$ onto \mathcal{J}^-

$$\langle \varphi^1, \varphi^2 \rangle = i \int_{\Sigma} d\sigma^{\mu} \left(\bar{\varphi}^1 \partial_{\mu} \phi^2 - \phi^2 \partial_{\mu} \bar{\varphi}^1 \right)$$
 (5.10)

Here, $d\sigma^{\mu}$ represents the future-directed surface element vector on Σ . This expression for the inner product is conserved and remains invariant under different choices of the Cauchy surface Σ . The conservation allows us to evaluate the integral on surfaces like The event horizon (H^+) and Future null infinity (\mathcal{J}^+) .

$$\langle \varphi^1, \varphi^2 \rangle = \langle \varphi^1, \varphi^2 \rangle_{H^+} + \langle \varphi^1, \varphi^2 \rangle_{\mathcal{J}^+}$$
 (5.11)

If Φ^{1+} and Φ^{2+} represent the projections of φ^1 and φ^2 onto \mathcal{J}^+ , then

$$\langle \varphi^1, \varphi^2 \rangle_{\mathcal{J}^+} = i \int_{\mathcal{J}^+} \left(\bar{\Phi}^1 \partial_\mu \Phi^2 - \Phi^2 \partial_\mu \bar{\Phi}^1 \right) du \, d\Omega \tag{5.12}$$

Where $d\Omega = \sin\theta \, d\theta \, d\phi$. from equation (5.9), (5.11) and (5.12), the following normalization conditions are valid for φ^{out}

$$\langle \varphi_J^{out}, \varphi_{J'}^{out} \rangle = -\langle \bar{\varphi}_J^{out}, \bar{\varphi}_{J'}^{out} \rangle = \delta_{JJ'}, \ \langle \varphi_J^{out}, \bar{\varphi}_{J'}^{out} \rangle = 0$$
 (5.13)

From this point onward, we adopt the notation $J = \ell, m, \omega$ and $J' = \ell', m', \omega'$,

$$\delta_{JJ'} \equiv \delta(\omega - \omega') \,\delta_{\ell\ell'} \,\delta_{mm'} \tag{5.14}$$

At this point, it is more practical to utilize wavepacket-type solutions, built from $\varphi_{\omega\ell m}$, as the basis functions rather than $\varphi_{\omega\ell m}$ themselves. These solutions are more localized in time and frequency, making them particularly useful for analyzing phenomena like Hawking radiation, where focusing on temporal localization near the event horizon of the black hole is essential. To proceed, we choose a

small positive real number δ (with $0 < \delta \ll 1$) and set $\epsilon = \delta \kappa$. (κ representing the surface gravity of the black hole), is introduced along with the following notation:

$$\varphi_{jn\ell m} = \epsilon^{-1/2} \int_{j\epsilon}^{(j+1)\epsilon} e^{2\pi i n\omega/\epsilon} \varphi_{\omega\ell m} d\omega \qquad (5.15)$$

In this context, j is a non-negative integer and n is any integer. From this point onward, we use the single symbol α to represent the collective index j, n, ℓ, m . We also introduce another family of solutions, $\varphi^{in}J$, characterized by their initial data (or images) on \mathcal{J}^- . The image Φ^-J of the solution on \mathcal{J}^- is defined analogously to the image on \mathcal{J}^+ , with the obvious substitution of the coordinate u by v.

$$\Phi_J^{in-}(v,\theta,\phi) = \frac{e^{-i\omega v}}{\sqrt{4\pi\omega}} Y_{\ell m}(\theta,\phi)$$
 (5.16)

We use the notation $\varphi^{in}\alpha$ to refer to the wavepackets formed from $\varphi^{in}j$ as defined in equation (5.15).

Let us now concentrate on late-time wavepackets φ_{α}^{in} , specifically those for which $n \geq N$ with $N \gg 1$, which represent certain high-frequency modes propagating in the spacetime outside a Schwarzschild black hole. This type of wavepacket originates from \mathcal{J}^- at advanced times v>0 and evolves entirely within the static Schwarzschild geometry. As it propagates, it reaches the peak of the effective potential barrier located near $r \approx 3M$. A portion of the wavepacket, denoted R_{α} , is reflected and escapes to future null infinity \mathcal{J}^+ , while the remaining part, T_{α} , transmits through the barrier and crosses into the event horizon. The reflected component appears on \mathcal{J}^+ as $R_{\alpha}\Phi^{out+}\alpha$. The transmitted portion, upon reaching the horizon H^+ , takes the form $T\alpha\varphi^{down}\alpha|H^+$, where $\varphi^{down}\alpha$ are wavepackets constructed from the so-called DOWN-modes $\varphi^{down}J$. These modes are defined by the condition that they vanish on \mathcal{J}^+ and take a specific form on the event horizon H^+ :

$$\varphi_J^{down}(v,\theta,\phi) = \frac{1}{\sqrt{4\pi\omega}} \frac{e^{-i\omega v}}{r_+} Y_{\ell m}(\theta,\phi)$$
 (5.17)

The late-time IN-, OUT-, and DOWN-modes, as defined above, are interconnected through the following relationship:

$$\varphi_{\alpha}^{in} = R_{\alpha}\varphi_{\alpha}^{out} + T_{\alpha}\varphi_{\alpha}^{down} \tag{5.18}$$

 φ_{α}^{out} : The OUT-mode, corresponding to radiation that escapes to infinity (\mathcal{J}^+) . φ_{α}^{down} : The DOWN-mode, corresponding to radiation absorbed into the black hole (H^+) . R_{α} and T_{α} are the **reflection amplitude** and **transmission (absorption) amplitude**, respectively. They quantify how much of the incoming wave is reflected or transmitted.

This closely corresponds to the relationships:

$$\varphi_J^{in} = R_J \varphi_J^{out} + T_J \varphi_J^{down} \tag{5.19}$$

This relation applies generally to eternal black holes. The J-subscript indicates a generic labeling of modes. It shows the same physical decomposition as in

Eq (5.18), meaning this is a universal property of wave propagation in such spacetimes. we also have

$$|R_{\alpha}|^2 + |T_{\alpha}|^2 = 1 \tag{5.20}$$

This equation ensures energy conservation for the wavepacket. he total energy of the wavepacket is distributed between the reflected component (escaping to J^+) and the absorbed component (falling into H^+).

We emphasize that, on a global scale, the geometry of an eternal black hole is distinct from that of a black hole formed through gravitational collapse. Consequently, the global behavior of the mode functions φ_J differs between these spacetimes. However, for wavepackets observed at late times, equation (5.18) holds in both cases. We now introduce a new family of modes, φ_{α}^{up} , defined by the condition that they are orthogonal to the φ_{α}^{in} modes, i.e. $\langle \varphi_{\alpha}^{up}, \varphi_{\alpha'}^{in} \rangle = 0$ These modes admit a decomposition of the form $\varphi_{\alpha}^{up} = t_{\alpha} \varphi_{\alpha}^{out} + r_{\alpha} \varphi_{\alpha}^{down}$, and are normalized such that $\langle \varphi_{\alpha}^{up}, \varphi_{\alpha'}^{up} \rangle = \delta_{\alpha\alpha'}$.

These conditions imply that the following relations hold:

$$|r_{\alpha}|^2 + |t_{\alpha}|^2 = 1, \quad t_{\alpha}\bar{R}\alpha + r_{\alpha}\bar{T}\alpha = 0$$
(5.21)

As the consequence of the relations (5.20) and (5.21), we have

$$|R_{\alpha}|^2 = |r_{\alpha}|^2, \quad |T_{\alpha}|^2 = |t_{\alpha}|^2$$
 (5.22)

The wavepacket φ_{α}^{up} , when traced backward in time, passes through a massive null shell before reaching past null infinity, \mathcal{J}^- . This process helps us trace the origins of the wavepacket from an earlier time. At \mathcal{J}^- , the wavepacket experiences **blueshifting** due to the black hole's gravitational field. The relation $u \sim \exp(\kappa u)$ shows this blueshift, with κ denotes the black hole's surface gravity and u and v are null coordinates.

Using the geometrical optics approximation, the evolution of the wavepacket is simplified. This approximation assumes that the wave behaves like light rays, which is valid in regions far from strong spacetime curvature. The result of this evolution is a wavepacket described by following equation

$$\Phi_{\omega\ell m}^{up-} = \frac{1}{\sqrt{4\pi\omega}} e^{-i\omega \ln(-\kappa v)/\kappa} Y_{\ell m}(\theta, \phi) \vartheta(-v)$$
 (5.23)

The step function ensures that the wavepacket Φ^{up-} is non-zero only for v < 0 representing its confinement to specific spacetime regions. The wavepacket φ_{α}^{up} generated at \mathcal{J}^- travels through the shell and moves through the potential barrier from within. The decomposition $\varphi_{\alpha}^{up} = t_{\alpha}\varphi_{\alpha}^{out} + r_{\alpha}\varphi_{\alpha}^{down}$ indicates that the wave is partially scattered by the potential barrier: the component $r_{\alpha}\varphi_{\alpha}^{down}$ falls into the black hole through the horizon, while the transmitted part $t_{\alpha}\varphi_{\alpha}^{out}$ It crosses the barrier and continues propagating toward past null infinity, \mathcal{J}^- (refer to Figure 5.1).

The last set of modes we require is represented by φ_{α}^{dn} . Their projections on \mathcal{J}^- , Φ_{α}^{dn-} are constructed by means of the transformation (5.15) from the following functions:

$$\Phi_{\omega\ell m}^{dn-}(v,\theta,\phi) = \bar{\Phi}_{\omega\ell m}^{up-}(-v,\theta,\phi) = \frac{1}{\sqrt{4\pi\omega}} e^{-i\omega\ln(-\kappa v)/\kappa} Y_{\ell m}(\theta,\phi) \vartheta(v)$$
 (5.24)

Asymptotic IN and OUT Mode Bases at Late Times

To formulate the in- and out-mode bases for late times, we introduce φ_{α}^{d} and φ_{α}^{p} which are formed as linear combinations of the modes φ_{α}^{up} and φ_{α}^{dn} ,

$$\varphi_{\alpha}^{d} = c_{\alpha}\varphi_{\alpha}^{dn} + S_{\alpha}\bar{\varphi}_{\alpha}^{up} , \quad \varphi_{\alpha}^{p} = c_{\alpha}\varphi_{\alpha}^{up} + S_{\alpha}\bar{\varphi}_{\alpha}^{dn}$$
 (5.25)

$$s_{\alpha} = w_{\alpha} (1 - w_{\alpha}^2)^{-1/2} , \quad c_{\alpha} = (1 - w_{\alpha}^2)^{-1/2}$$
 (5.26)

where $w_{\alpha} = exp[-\pi\omega_{j}/\kappa]$. These combinations are introduced because, in the context of curved spacetimes, solutions behave differently depending on the causal structure of spacetime (e.g., near null infinities \mathcal{J}^{-} or \mathcal{J}^{+}). The objective is to represent the field using mode functions that are well-defined in the late-time region \mathcal{J}^{-} , corresponding to the 'in' and 'out' solutions. The modes φ_{α}^{d} and φ_{α}^{p} are chosen to correspond to solutions with positive frequency relative to the advanced time coordinate v, thereby ensuring a physically meaningful interpretation in terms of particle states. These functions are derived by applying the transformation (5.15) to solutions that exhibit a specific dependence on v at \mathcal{J}^{-} :

$$F_{\omega\ell m}(v) = \theta(v)e^{-iq\ln\kappa v} + \theta(-v)e^{-\pi q}e^{-iq\ln(-\kappa v)}$$
(5.27)

In this expression, the parameter q is defined for D-modes as $q = \omega/\kappa$, while for P-modes, it is $q = -\omega/\kappa$. The function $F_{\omega\ell m}(v)$, defined for the full range $-\infty < \omega < \infty$, contains only positive frequency components with respect to the advanced time coordinate v. Accordingly, we select the following positive-frequency solutions as our in-mode basis:

$$\Phi_{\alpha}^{\text{in}} = \begin{pmatrix} \varphi_{\alpha}^{\text{in}} \\ \varphi_{\alpha}^{\text{d}} \\ \varphi_{\alpha}^{\text{p}} \end{pmatrix} \tag{5.28}$$

with $\alpha = \{j, n, \ell, m\}$ and $n \geq N$, and augment them to a complete orthonormalized basis with an arbitrary set of positive-frequency functions defined on \mathcal{J}^- . Likewise,

we form the out-basis by augmenting the set of functions

$$\Phi_{\alpha}^{\text{out}} = \begin{pmatrix} \varphi_{\alpha}^{\text{out}} \\ \varphi_{\alpha}^{\text{down}} \\ \varphi_{\alpha}^{\text{dn}} \end{pmatrix}$$
(5.29)

forming a complete orthonormal system. Comparable sets of basis functions were originally introduced by Wald (1975). In the following discussion, we will refer to equations (5.28) and (5.29) as **Wald's bases**.

The modes $\Phi_{\alpha}^{\text{in}}$ correspond to positive-frequency solutions relative to advanced time v at past null infinity \mathcal{J}^- . In the associated 'in-vacuum' state, no particles are present incoming from \mathcal{J}^- , effectively describing a scenario in which the black hole initially exists in isolation, unaffected by external radiation. Conversely, the modes $\Phi_{\alpha}^{\text{out}}$ represent positive-frequency solutions with respect to the retarded time u at future null infinity \mathcal{J}^+ . The corresponding 'out-vacuum' state then represents a configuration with no outgoing particles reaching \mathcal{J}^+ . This models the state in which the black hole emits no radiation in its final

stages. The particle interpretation is well-defined at \mathcal{J}^- (incoming particles) and \mathcal{J}^+ (outgoing particles) because the spacetime in these asymptotic regions is weakly curved and resembles flat spacetime. This allows the use of standard quantum field theory concepts like positive frequency and vacuum states. The modes $\varphi_{\alpha}^{\text{down}}$ and $\varphi_{\alpha}^{\text{dn}}$ which vanish at \mathcal{J}^+ , are not associated with a straightforward particle interpretation. They correspond to regions closer to the event horizon or in highly curved spacetime.

In the general scenario, the Bogoliubov coefficient matrices that connect the in- and out-bases are infinite-dimensional. However, for Wald's bases, these matrices factorize, effectively reducing the problem to a three-dimensional one. While these modes lack a straightforward particle interpretation at \mathcal{J}^+ , their specific choice has no bearing on the physical predictions made in the black hole's exterior region. This simplification is critical because it allows the focus to remain on the regions of physical interest (e.g., near the black hole horizon and at infinity).

Black Hole Thermodynamics

One of the most well-known facts about black holes is that crossing their event horizon is a one-way journey— with nothing, not even light, can escape once it has passed this boundary. In other words, **entering a black hole is an irreversible process**. This irreversibility is in obvious tension with basic physical principles. For example, many fundamental physical laws (e.g., Newtonian mechanics, Maxwell's equations, Schrodinger's equation in quantum mechanics) are symmetric with respect to time. i.e if a process is allowed in one direction then this laws also permits the exact reverse process to occur. On the other hand, irreversibility is very familiar to everyday life scenarios, such as breaking of glass or heat flowing from hot to cold do not reverse themselves.

Classical physicists saw some tension between such irreversibility and a presumed invariance of the laws of nature under time-reversal. The tension was largely resolved with the development of thermodynamics and statistical mechanics. Irreversible processes are those in which the entropy increases. Processes in which the entropy becomes smaller – for example, a scrambled egg spontaneously reassembling - can happen in principle but require extreme fine-tuning of initial conditions, so they are exponentially unlikely. The core concept of black hole thermodynamics is that the irreversible nature of an object being absorbed by a black hole mirrors the statistical irreversibility we observe in everyday physics. When an object falls into a black hole, the system's entropy increases, making the process fundamentally one-directional. While it is theoretically possible for the black hole to spontaneously emit the same object in a time-reversed scenario, this would require extremely precise starting parameters, making it nearly impossible—much like how a shattered egg never reassembles itself on its own. Black hole thermodynamics has raised many challenging questions about the fundamental nature of quantum mechanics and gravity.

Black Hole Entropy And The Generalized Second Law

The second law of Thermodynamics says that, in any process that we can observe in practice, the entropy is non-decreasing. Here, entropy is the usual thermodynamic entropy. Processes in which the thermodynamic entropy decreases are allowed by the laws of nature, but are prohibitively unlikely, in practice. However, Bekenstein was inspired by a question from his supervisor, John Wheeler, which made him think about what happens to the entropy when matter falls into the black hole. Thought experiment with tea and black hole: If a cup of tea (representing a system with entropy) is thrown into a black hole, the entropy of the tea seems to disappear. Traditionally, black holes were thought to have **zero entropy**, so the total entropy of the universe would appear to decrease. The second law of thermodynamics states that the total entropy of a closed system should never decrease. However, the apparent disappearance of tea's entropy in this scenario would violate this fundamental law. To preserve the Second Law, Bekenstein proposed assigning entropy to black holes themselves. He theorized that this entropy should always increase when matter (and its entropy) falls inside the Black hole according to classical General Relativity, ensuring that the Second Law holds true. Which property of a black hole can only grow? The mass of a black hole does not always increase— For instance, a spinning black hole can lose mass as its rotation slows down. However, there is a quantity that continually grows. Hawking had just proven the "Area Theorem", this principle states In the framework of classical general relativity, black hole horizons never contract. Bekenstein, therefore, postulated that a black hole's entropy is linked to the size of its horizon. The horizon is situated at the Schwarzschild radius $r_s = 2GM$ and the horizon area is given by :

$$A = 4\pi r_s^2 = 16\pi G^2 M^2 \tag{7.1}$$

Since, the entropy is dimensionless, So, if the black hole's entropy is to be directly proportional to its horizon area, the constant of proportionality will have units of Inverse Area. Using the fundamental constants c, G, and \hbar one can derive the Planck length $l_p = (\hbar G/c^3)^{1/2}$ and the plank area $l_p^2 = \hbar G/c^3$. In units with c = 1, Bekenstein's formula for entropy of black hole was:

$$S = \frac{A}{4G\hbar} \tag{7.2}$$

where the constant 1/4 was not clear in Bekenstein's work and was determined by Hawking a couple of years later. The formula with this factor of 1/4 included is commonly called the **Bekenstein-Hawking entropy** of the black hole. According to equation (7.2), Black hole entropy can reach exceptionally high values compared to everyday systems. for example, a black hole with the mass of the sun has an entropy of roughly 10^{77} , which is about 10^{18} times the entropy of the actual sun. (we set $\hbar=1$ in later discussion). Bekenstein suggested that the entropy of a black hole reflects the number of different configurations that could have led to its formation. He introduced the concept of **generalized entropy**, which combines the entropy of the black hole itself—given by (A/4G) with the external entropy (S_{out}) , representing the entropy of matter and radiation located outside the event horizon. The generalized entropy is given by:

$$S_{\rm gen} = \frac{A}{4G} + S_{\rm out} \tag{7.3}$$

The generalized entropy was proposed to obey a generalized second law, i.e. it is non-decreasing in all the processes that we can observe in practice.

$$\frac{dS_{\text{gen}}}{dt} \ge 0 \tag{7.4}$$

Bekenstein tested the validity of the generalized second law in scenarios involving Schwarz-schild black holes. the main idea was to test whether the generalized second law (7.4) is valid when the black hole absorbs matter. The law assumes that the matter being absorbed by the black hole should obey the thermodynamic principles, i.e. it is near local thermal equilibrium. A simple case to consider is that the black hole absorbs a beam of black body radiation, say at temperature T. In 3+1 dimensions, the relation between energy (E), temperature (T) and entropy (S) in black body radiation is $E = \frac{3}{4}TS$. If a black hole of mass M absorbs energy E << M from black body radiation, its entropy $A/4G = 4\pi GM^2$ increases by $8\pi GME$, while the entropy of the radiation decreases by $\Delta S_{\rm out} = 4E/3T$. Thus, change in generalized entropy is:

$$\Delta S_{\rm gen} = \left(8\pi GM - \frac{4}{3T}\right)E\tag{7.5}$$

 $\Delta S_{\rm gen}$ becomes negative if T is so small that the typical photon wavelength is much larger than the Schwarzschild radius. From a thermodynamic perspective, given that Bekenstein assumed a black hole does not emit radiation, it must be assigned a temperature of zero. As per thermodynamics, in a state of equilibrium, the variations in energy E and entropy S of a system are connected as: dE = TdS or dS = dE/T. A system at T = 0 should exhibit $dS = \infty$ if $dE \neq 0$, according to thermodynamics. However, Bekenstein aimed to assign a finite, rather than infinite, entropy to the black hole.

Black Hole Evaporation

Penrose diagram are usually drawn for spherically symmetric spacetime. The main purpose of this diagram is to exhibit causal relations in a useful way. The diagram is drawn so that radially ingoing or outgoing null geodesics are at a $\pi/4$ angle to the vertical. An important example is a Penrose diagram describing spherically symmetric collapse of a star to a Schwarzschild black hole (Fig 8.1). The left vertical boundary of the figure is the origin of Polar coordinates at r=0. shown in red is the worldvolume of a star. The star ends its life at the singularity represented by the wiggly line at the top of the diagram, Future and past null infinity are represented by diagonal lines on the right boundary. The diagonal line within the figure represents the event horizon of the black hole. Since, causal curves travel at an angle no greater than $\pi/4$ from the horizon, an observer outside the horizon can never see beyond (on the other side of) the horizon. The Worldline of a massive observer who remains forever outside the horizon (and does not accelerate indefinitely) will end at the point i^+ , known as future infinity, where the horizon and future null infinity meet.

Hawking's discovery of black hole evaporation was derived from analyzing the behavior of a quantum field within a fixed classical background, specifically a Schwarzschild black hole with mass M, which is a reasonable approach approximation if M is much bigger than the Planck mass $(\hbar c/G)^{1/2}$, which is about 10^{-5} grams. Moreover, it is potentially a sensible approximation if the Schwarzschild radius of the black hole is much bigger than the Planck length $(\hbar G/c^3)^{1/2} \approx 10^{-33}$

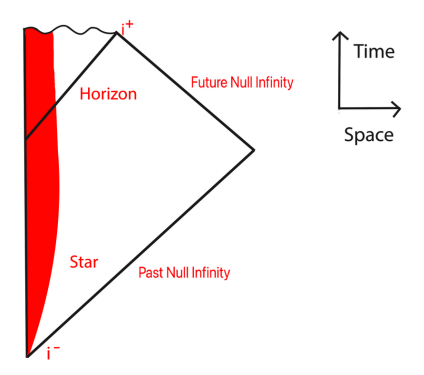


Figure 8.1: A Penrose diagram describing the collapse of a star to form a black hole.

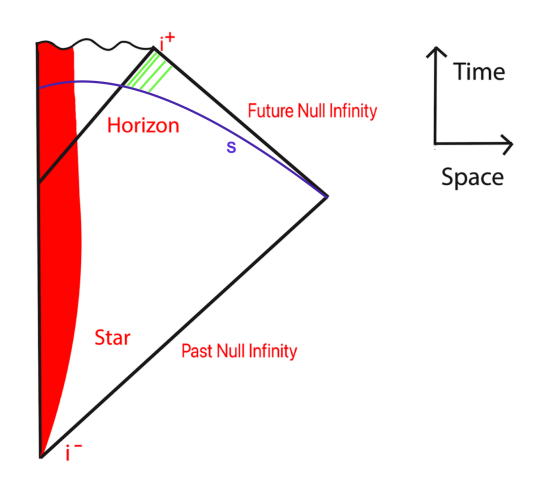


Figure 8.2: Whatever the distant observer sees in the far future can be traced back to initial conditions on a Cauchy hypersurface, such as the hypersurface S shown in violet. This Cauchy hypersurface has been chosen to cross the horizon outside the worldvolume of the collapsing star. From this Cauchy hypersurface, signals can propagate to the distant observer at the speed of light. These signals can propagate along outgoing null geodesics, some of which are indicated by the green lines in the figure, which are at a $\pi/4$ angle to the vertical. These outgoing null geodesics, if labeled by the time of a distant observer, "bunch up" near the horizon, as shown, because the redshift diverges there.

cm. For a realistic astrophysical black hole, Hawking approximation is expected to be excellent.

Our aim is to analyze what an observer far from the collapsing star will see in the far future, after the transients have died out. As an ideal case, we assume that what are observed are massless fields such as the electromagnetic field, and these are observed at future null infinity, more specifically near the upper boundary of null infinity where it ends at the point i^+ . These conditions are comparable to making observations either far from the black hole or at a much later time.

Measurements that the observer will make at, or near, future null infinity can be traced back to initial conditions on a Cauchy hypersurface. For this purpose we can choose any Cauchy hypersurface we want. It is convenient to choose one that crosses the horizon outside the collapsing star such as the hypersurface S of (Fig 8.2). From any point on S, a massless particle might be emitted and propagate to future null infinity at the speed of light. The diagonal green lines in the diagram represents the trajectories of such particles. Let u be any coordinate function used to describe a location near the black hole in terms of its distance from the event horizon. u vanishes on the event horizon (u=0) and is positive outside the event horizon (u > 0) (where signals can still escape). The normal derivative of u (a measure of how u changes along the horizon's surface) is assumed to be non-zero and finite; i.e. u changes predictably near the horizon and is a useful coordinate for analysis. A signal (E.g light or radiation) emitted near the Black hole's vicinity can originate at any location defined by u. A signal emitted close to the event horizon will have a small u, while a signal released farther away from the black hole will have a larger u. Let t be the time at which

the distant observer receives the signal. The relation between t and u is :

$$t = 4GM \log\left(\frac{1}{u}\right) + C + \mathcal{O}(u) \tag{8.1}$$

Where C is a constant that depends on how far the observer is and is the precise definition of the function u. Equation (8.1) tells us that as $u \to 0^+$, the time t at which the signal is received by a distant observer diverges, but only logarithmically. Indeed, this divergence is related to the fact that a signal that originated from behind the horizon say at u < 0, will never reach the outside observer. Solving (8.1) to express u in terms of t for asymptotically large t we get:

$$u = e^C e^{-t/4GM} \tag{8.2}$$

At late times, i.e. if t is large, u is exponentially small, this means that the observations are effectively probing regions closer and closer to black hole's event horizon, or in other words, at late time measurements by the distant observer probe the quantum state at distances exponentially close to the horizon. Quantum Field Theory predicts that, at extremely short distances, any state appears similar to the vacuum. As a result, what a distant observer sees at late times essentially reflects vacuum behavior at exponentially tiny distances. The distant observer does not need to wait terribly long before making observations that probe vacuums state at short distances. The term $e^{-t/4GM}$ shows that u decreases exponentially as t increases. The parameter 4GM determines the timescale of this decay. For example, a Solar mass black hole $(M \approx 2 \times 10^{30} \text{ Kg})$, 4GM corresponds to a time about 2×10^{-5} Seconds.

This decay factor $e^{-t/4GM}$ becomes incredibly small even for relatively small values of t. For example, after waiting just 1 second, the factor becomes e^{-50000} or $e^{-5\times10^4}$, which reduces u by extremely small amount. Hence, the observer need not to wait very long (in human timescale) to reach by the late time regime. The distant observer probes the radiation emerging from the black hole by measuring a quantum field Ψ . We assume that the distant observer measure Ψ as a function of time (t) and angular coordinate Ω at a fixed spatial distance from the black hole. A typical observable quantity for the observer is a two-point function given as:

$$\langle \Psi(\Omega, t) \Psi(\Omega', t') \rangle \tag{8.3}$$

This two point function provides information about the structure and dynamics of the quantum field over time and angular positions. In a spherically symmetric Schwarzschild background the field Ψ can be expanded into Partial Waves. The coefficient of each partial wave is a 1+1 dimensional quantum field (one spatial dimension and one time). In real world scenario, the field Ψ could represent a component of the Electromagnetic field, the expansion would involve vector spherical harmonics. We can understand the essence of Hawking's discovery by assuming that a specific partial wave ψ of the field Ψ behave like a chiral free fermion in 1+1 dimensional spacetime.

The fermion is described as chiral in the above statement because it represents only the outward propagating modes (from event horizon to infinity). These modes are crucial for modeling the Hawking radiation that escapes the black hole, while the inward modes are irrelevant since they do not contribute to the observable radiation. Thus, this choice of focusing on chiral fermions simplifies the analysis while still capturing the essence of the physical process. A chiral free fermion in 1+1 dimensions has scaling dimension 1/2, and its two-point function in the vacuum is:

$$\langle \psi(u)\psi(u')\rangle = \frac{(dudu')^{1/2}}{u - u'} \tag{8.4}$$

In the analysis of black hole emission in the late-time regime, u and u' are both exponentially small and therefore exponentially close to each other. Since we know that any state looks like the vacuum state at sufficiently short distances, so in discussing what an observer will see at late times, we can replace $\langle \psi(u)\psi(u')\rangle$ by its vacuum expectation value (8.4). Substituting (8.2) in (8.4), we can turn equation (8.4) into a formula for the two-point function by the distant observer at late times:

$$\langle \psi(t)\psi(t')\rangle = \frac{1}{4GM} \frac{(dtdt')^{1/2}}{e^{(t-t')/8GM} - e^{-(t-t')/8GM}}$$
 (8.5)

Equation (8.5) describes a two point function $\langle \psi(t)\psi(t')\rangle$, in context of a black hole's thermal behavior. This two point function is antiperiodic in imaginary time, i.e. the function exhibits a repeating behavior under a shift $t \to t + 8\pi GMi$; where $8\pi GM$ represents a specific periodicity linked to the black hole's thermodynamic properties. Anti-periodicity with that period corresponds to a thermal correlation function at a temperature $T_H = 1/8\pi GM$, referred to as "Hawking Temperature" of a Black Hole. It is the temperature at which a Black Hole emits thermal radiation due to quantum effects near the event horizon. The right hand side of equation (8.5) is interpreted as two-point correlation function of a quantum field (a chiral free fermion) at the Hawking temperature T_H . A two-point function is a mathematical tool to understand correlations between values of field $\psi(t)$ at different times t and t'. The correlation function arises in the thermodynamic limit, which is expressed as:

$$\frac{1}{Z} Tr e^{-\beta_H H} \psi(t) \psi(t')$$

Where, Z is a Partition function, representing the statistical properties of the system. H is a Hamiltonian, governing system's energy. $\beta_H \to 1/T_H$ is inverse of temperature. The thermal two-point function is unique and determined by the facts: It is Antiperiodic with period $8\pi GMi$ and it's only singularity occurs when t=t', at which point the function has a simple pole with residue 1. A Black hole's observations as perceived by a faraway observer at late times align with what would be expected if the black hole were a thermal system. specifically, the Black hole emits radiation similar to a Black body at temperature $T_H = 1/8\pi GM$, this thermal reaction is known as Hawking Radiation.

When a Black hole forms, transient effects initially dominate the radiation over time, these transients fade and the reaction becomes predominantly thermal characterized by Hawking Temperature T_H . This explains why Bekenstein struggled with understanding how black holes interact with photons of energy much smaller than $1/8\pi GM$ (very low energy photons). These low-energy photons are significant because the black hole strongly emits them due to its thermal

nature and each mode of the radiation has a large average occupation number (a measurement of the quantity of photons within that state), making the emission prominent. When examining a Black hole's radiation emission, the increase in the radiation's entropy must be accounted for the generalized second law. Low-energy photons contribute significantly to the increase in entropy because of their high occupation number. We can also now confirm Bekenstein's formula for the Black hole's entropy, and explain how Hawking determined the overall constant in this formula. We use the first law of thermodynamics:

$$dE = TdS (8.6)$$

Where the energy is the black hole mass M, and for Schwarzschild black hole $T = 1/8\pi GM$. Hence, $dS = 8\pi GMdM$ (assuming that S vanishes if there is no black hole, i.e. at M = 0), so $S = 4\pi GM^2$. The Schwarzschild black hole's area is $A = 16\pi G^2M^2$, so the entropy is:

$$S = \frac{A}{4G} \tag{8.7}$$

This is how Hawking confirmed Bekenstein's ansatz and determined the overall normalization. One way to justify equation (8.1) and (8.2) is to introduce the Kruskal-Szekeres coordinates. A standard definition is:

$$U = -\left(\frac{r}{2GM} - 1\right)^{1/2} e^{r/4GM} e^{-t/4GM}$$

$$V = \left(\frac{r}{2GM} - 1\right)^{1/2} e^{r/4GM} e^{t/4GM}$$
(8.8)

In terms of these coordinates the Schwarzschild metric is:

$$ds^{2} = -\frac{32G^{3}M^{3}}{r}e^{-r/2GM}dUdV + r^{2}d\Omega^{2}$$
(8.9)

Where r is defined implicitly as:

$$-UV = \left(\frac{r}{2GM} - 1\right)e^{r/2GM} \tag{8.10}$$

The most important application of Kruskal-Szekeres coordinates is to describe the extension of the Schwarzschild geometry beyond the horizon at r=2GM. These coordinates make the metric regular across the event horizon (r=2GM) and remove the singularity that appears in Schwarzschild coordinates at this radius. The form of the metric in equation (8.9) shows that a radially outgoing or incoming null geodesic $(ds^2=0)$ must satisfy dU=0 or (dV=0), so in other words U or V is constant along such geodesic. In the outgoing direction, U does not change or is constant because it encodes the behavior of light escaping from the black hole. Whereas, in the incoming direction, V does not change or is constant because it encodes the behavior of light falling towards the black hole. Equation (8.8) shows that U vanishes at r=2GM and is negative for r>2GM, so for a function that vanishes on the horizon and is positive outside, we take u=-U. From equation (8.8) then gives the claimed result $u=Ce^{-t/4GM}$ (i.e. (3.2)), where $C=\left(\frac{r}{2GM}-1\right)^{1/2}e^{r/4GM}$ is a constant that depends on the position

of the observer and not on the time at which the observation is made. Now, it is natural to introduce the retarded time $t_{ret} = t - r$ and write the formula for u in the form :

$$u = \left(\frac{r}{2GM} - 1\right)^{1/2} e^{t_{ret}/4GM} \tag{8.11}$$

For a black hole with solar mass, $4GM \approx 2 \times 10^{-5} Sec$ the exponential dependence of u on t_{ret} ensures that u becomes negligible for large t_{ret} , consistent with the behavior expected in black hole spacetimes. An important detail in this derivation os that it is not necessary to begin the discussion at distances so small, or energies so high that they probe the unknown physics (quantum gravity at plank scale). Instead, the approach assumes that at late times, the observable effects seen by the distant observer can be explained by considering the short distance behavior of the quantum field, but only in context of known physics. The term short distances here does not refer to plank scale or other extremely small scales beyond our current understanding.

The hypersurface S is chosen so that the signal originates from a region close to the black hole (small compared to the Schwarzschild radius) but still far enough that the fine details of the black hole's geometry does not affect the core correlation function $\langle \psi(u)\psi(u')\rangle$, which coincides with the expectation value in vacuum. So, for example, For an Astrophysical Black hole, with Schwarzschild radius of a few kilometers or more, the short distance scale could be a millimeter; significantly smaller than the size of the black hole, but not nearly small enough to probe the limits of our knowledge of physics. The Hawking Temperature $T_H = 1/8\pi GM$ can be expressed in terms of the Schwarzschild radius $r_s = 2GM$ as:

$$T_H = \frac{1}{4\pi r_s} \tag{8.12}$$

Thus, the Hawking Temperature is of order $1/r_s$ and a typical massless particle (Eg: Photons) emitted by the black hole has a wavelength measured at infinity of order r_s and an energy of order $1/r_s$. Energy loss by a radiating astrophysical black hole is extremely small. the total luminosity of a radiating body of surface area A and temperature T is of order AT^4 , which in the case of a black hoke is a multiple of $1/G^2M^2$. Thus, in order of magnitude the energy loss rate of a radiating Astrophysical Black hole is:

$$\frac{dM}{dT} \sim \frac{1}{G^2 M^2} \tag{8.13}$$

With the real world assumptions about the particles emitted by the black hole mainly photons and gravitons the constant of proportionality in equation (8.13) was computed by page. (This calculations require understanding of gray body factors, which we will introduce in the next chapter). Following Hawking, energy loss by a radiating Black Hole is known as "Black Hole Evaporation". Equation (8.13) indicates that a Black Hole with a standard astrophysical mass evaporates extremely slowly. The duration for the Solar-Mass Black Hole in vacuum to evaporate away a significant part of its mass is of order 10⁶⁷ years. Of course, in the real world, an astrophysical black hole is not in vacuum and is more likely to accrete mass than to evaporate. Hawking's calculations shows that black hole emit radiation with Thermal spectrum, implying that outgoing radiation carries no information about the matter that originally formed the black

hole. This presents a puzzle because if the black hole initially formed from a pure quantum state, quantum mechanics dictates that the final state after evaporation should also be pure.

The radiation has a large entropy, roughly proportional to the number of photons emitted during evaporation. For example, for a solar mass black hole, this entropy is about 10⁷⁶. However, according to Unitary evolution in quantum mechanics, information should be preserved, leading to the paradox. The thermal appearance of Hawking radiation arises because a distant observer only has access to the quantum fields outside the event horizon. Even if the whole universe remains in a pure state, the portion of spacetime observed outside the black hole appears as a mixed state. This suggests that the missing information could be encoded in the correlations between the emitted radiation and the hidden regions inside the black hole, which remain inaccessible to an external observer. This is the essence of the Hawking effect.

Chapter 9

Gray Body Factors

In the previous section, we saw that a signal emitted from the horizon propagates freely to distant observer. However, this assumption is oversimplified, since in general there is a sort of angular momentum barrier around the black hole. As we will see an outgoing signal might be reflected back towards the horizon. Now, it is possible in 3+1 dimensions to have a semi-realistic model. For this we consider a magnetic charged black hole and a massless electrically charged fermion field Ψ interacting with the black hole. The Partial wave of Ψ of lowest possible angular momentum is as massless fermion in 1+1 dimensional sense, and its outgoing (chiral) component has precisely the properties assumed in the previous section for a study of such models. Also there is a potential barrier outside the black holes. (even for angular momentum zero).

9.1 The Potential Barrier

For simplicity, we will consider a massless scalar field ϕ in the presence of the black hole. In the real world, it would be more realistic to consider the EM field or gravitational field. We assume that ϕ interacts with gravity only, with minimal coupling via the action $-\frac{1}{2}\int d^4x\sqrt{g}g^{\mu\nu}\partial_{\mu}\phi\partial_{\nu}\phi$. In a Schwarzschild background, the action for a mode of angular momentum l is :

$$I = \int dt \, dr \left(\frac{r^2}{2} \frac{1}{1 - \frac{2GM}{r}} \left(\frac{d\phi}{dt} \right)^2 - \frac{r^2}{2} \left(1 - \frac{2GM}{r} \right) \left(\frac{d\phi}{dr} \right)^2 - \frac{l(l+1)}{2} \phi^2 \right)$$
(9.1)

Where, the first term corresponds to Kinetic energy in time. The second term represents spatial Kinetic energy in radial direction. The third term acts as an angular potential term due to the angular momentum l. It is useful to define the "Tortoise coordinate" $r_* = r + 2GM \log(r - 2GM)$, which satisfies $dr = dr_* \left(1 - \frac{2GM}{r}\right)$, and ranges over the whole line $-\infty < r_* < \infty$ for $2GM < r < \infty$. The Tortoise coordinate allows for a better analysis of wave propagation in the black hole background. The action (9.1) is rewritten in terms of r_* as:

$$I = \int dt \, dr \left(\frac{r^2}{2} \left(\frac{d\phi}{dt}\right)^2 - \frac{r^2}{2} \left(\frac{d\phi}{dr_*}\right)^2 - \left(1 - \frac{2GM}{r}\right) \frac{l(l+1)}{2} \phi^2\right) \tag{9.2}$$

Setting $\phi = \sigma/r$ and integrating by parts, we get :

$$I = \int dt \, dr_* \left(\frac{1}{2} \left(\frac{d\sigma}{dt} \right)^2 - \frac{1}{2} \left(\frac{d\sigma}{dr_*} \right)^2 - \left(1 - \frac{2GM}{r} \right) \left(\frac{l(l+1)}{2r^2} + \frac{GM}{r^3} \right) \sigma^2 \right)$$

$$(9.3)$$

In other words, σ is effectively a massless scalar propagating in effective two-dimensional Minkowski space with line element $-dt^2 + dr_*^2$ and interacting with the effective potential:

$$V_{\text{eff}} = \left(1 - \frac{2GM}{r}\right) \left(\frac{l(l+1)}{2r^2} + \frac{2GM}{r^3}\right)$$
(9.4)

The effective potential is positive definite, vanishing near the horizon and at infinity, with a barrier in between. Even if l=0, there is a non-trivial effective potential namely:

$$V_{\text{eff}} = \frac{2GM}{r^3} - \frac{4(GM)^2}{r^4} \tag{9.5}$$

The maximum value of this potential is at $r_{\rm max}=\frac{8}{3}GM$, and it's corresponding value is $V_{\rm max}(l=0)=\frac{27}{1024(GM)^2}$. For l>0, the maximum of potential is greater. For large l, the maximum is approximately at r=3GM, and the maximum value of the potential is $V_{\rm max}(l)\cong\frac{l(l+1)}{27(GM)^2}$. To get from horizon to infinity, a wave will have to propagate over the potential barrier. Only a wave whose energy is much greater than $\sqrt{V_{\rm max}(l)}$ will propagate almost freely from the horizon at $r_*=-\infty$ through the barrier to $r_*=\infty$. Our previous calculations are good for l=0 mode if the black hole's Hawking radiation is being observed at frequencies much above the Hawking Temperature $T_H=\frac{1}{8\pi GM}\approx \sqrt{V_{\rm max}(l=0)}$. For l>0, the previous calculations is good at frequencies much above $l\,T_{\rm max}$.

An outgoing mode from the horizon at $r_* = -\infty$ might be scattered back into the black hole by the potential and reabsorbed, or it might be transmitted across the barrier to $r_* = \infty$. Our calculations in the previous section should be modified accordingly; The probability to observe an outgoing particle near $r_* = \infty$ should be reduced by the transmission probability across the barrier. If a black hole has a temperature T_H , it can theoretically reach equilibrium with a thermal gas at that temperature. In this state, the black hole absorbs thermal radiation from the gas and emits its own thermal radiation at the same temperature, maintaining a balance. In the simplest case, where there is no effective potential barrier (A situation that only happens for an electrically charged massless fermions interacting with a magnetic charged Black Hole), A Black Hole absorbs all the incident radiation in a particular partial wave. With no barrier present, the Black hole freely emits radiation while remaining in equilibrium. In a more realistic situation, an effective potential barrier $(V_{\text{eff}} \neq 0)$ exists. This barrier reduces the probability of the black hole absorbing radiation. The absorption probability is reduced by a factor equal to the transmission probability from right to left (i.e. from $r_* = \infty$ to $r_* = -\infty$). To maintain equilibrium, the emission probability of radiation from the black hole must also be reduced by the same factor. Thus, the transmission probability through the barrier is same in both directions (left to right and right to left). Therefore, equilibrium is possible if the black hole's emission is adjusted by this transmission probability factor.

The statement that the transmission probability of a wave through a potential barrier is same whether the wave is incident from left or right can be proved as follows. A solution of Klein-Gordon equation for σ with frequency ω has the form $\sigma(r_*,t) = \lambda(r_*) e^{-i\omega t}$ with:

$$\left(-\frac{d^2}{dr_*^2} + V_{\text{eff}}(r_*)\right)\lambda(r_*) = \omega^2 \lambda(r_*)$$
(9.6)

A solution λ_{ω} that describes the scattering of a wave incident from the left has the asymptotic behavior:

$$\lambda_{\omega}(r_*) \sim \begin{cases} e^{i\omega r_*} + R(\omega) e^{-i\omega r_*}, & r \to -\infty \\ T(\omega) e^{i\omega r_*}, & r \to +\infty. \end{cases}$$
(9.7)

Where, $T(\omega)$ and $R(\omega)$ are the transmission and reflection amplitudes for a wave incident from the left. A solution $\tilde{\lambda_{\omega}}$ that describe the scattering of a wave incident from the right has the asymptotic behavior:

$$\tilde{\lambda}_{\omega}(r_*) \sim \begin{cases} \tilde{T}(\omega) e^{-i\omega r_*}, & r \to -\infty \\ e^{-i\omega r_*} + \tilde{R}(\omega) e^{i\omega r_*}, & r \to +\infty. \end{cases}$$
 (9.8)

Where, $\tilde{T}(\omega)$ and $\tilde{R}(\omega)$ are the transmission and reflection amplitudes for a wave incident from the right. Since, both λ_{ω} and $\tilde{\lambda_{\omega}}$ satisfy the same equation (9.6), their Wronskian $\lambda_{\omega} \frac{d}{dr_*}$ is independent of r_* . Comparing the values ar $r_* \to \pm \infty$, we get the claimed result $T(\omega) = \tilde{T}(\omega)$.

9.2 More Detailed Argument

Now, we will aim for more technical/mathematical justification of the claim that the thermal radiation rate found in previous section must be multiplied by a factor $|T(\omega)|^2$. In simple terms, the observer is trying to measure radiation from the black hole. To describe what the observer detects, we need a mathematical operator that represents the measured quantity. The goal is to define a operator in a way that make sense physically and allows us to calculate what is observed. In QFT, physical quantities (like energy, momentum or radiation flux) are represented by "operators" acting on quantum field. Here, the operator W is defined as:

$$W = \int_{S'} d^3x \sqrt{h} \left(a(x) \sigma(x) + b(x) \dot{\sigma}(x) \right)$$
(9.9)

Where, S' is a Cauchy hypersurface; which is just a fancy term for a 3D slice of spacetime where we specify initial data for quantum field. h is the induced metric on S' which describes the geometry of this spacetime. $\sigma(x)$ is quantum field at point x. $\dot{\sigma}(x)$ is the time derivative of $\sigma(x)$; describing how the fields evolve in time. Finally, a(x) and b(x) are functions that weight the contributions of $\sigma(x)$ and $\dot{\sigma}(x)$ to the operator W. W is an operator that combines the field σ and its time derivative $\dot{\sigma}$ on the hypersurface S'. If we measure $W^{\dagger}W$, we obtain the number of particles at a given energy. The observer detects particle corresponding to this operator. It is useful to select the hypersurface S' to pass

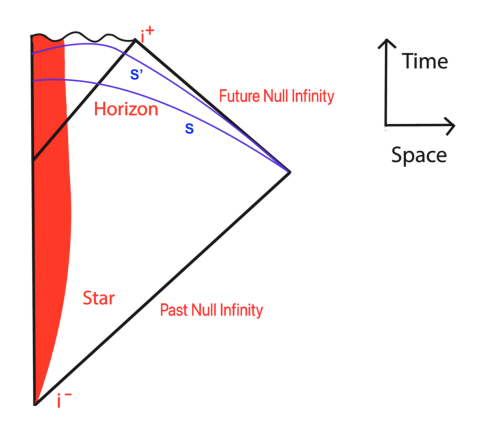


Figure 9.1: This picture illustrates a more detailed derivation of the Hawking process. S' is a late time Cauchy hypersurface on which a measurement will be made. The operator that will be measured is $W^{\dagger}W$, where W is a linear function of a quantum field σ and its time derivative $\dot{\sigma}$ on the surface S'. By solving the wave equation backwards in time, starting with "final data" on S', one can obtain an expression for W in terms of σ and $\dot{\sigma}$ on an earlier hypersurface S. This leads to a corrected prediction for black hole radiation that incorporates the interaction between the outgoing radiation and the gravitational field of the black hole.

through the detector at the time of measurement. Since, the measurement is taken far away from the black hole, where the observer is located. We want to describe the field in terms of what the detector will measure, not just in terms of initial conditions. The function a(x) and b(x) should be localized near the detector, i.e. they are non-zero only in the region where the measurement occur. If we choose S' correctly, The operator W will describe the field in a way that matches what the detector measures. This ensures we correctly count the number of Hawking radiation particles detected. Because the observer's detector is positioned far from the black hole, it is necessary to describe the field in that distant region. By choosing S' to be well into the future, we ensure we capture the outgoing radiation. The measurement at S' will be related to earlier field values at S through the wave equation.

The function W needs to be constructed carefully to represent physical particle detector. The function a(x) and b(x) should behave like plane wave $(e^{i\omega t})$ to match the frequency modes the detectors measures if chosen correctly, W behaves as an "Annihilation operator" for a given frequency ω ; while its conjugate W^{\dagger} is a "Creation operator". The quantity $W^{\dagger}W$ tells us how many particles exists at a given energy ω . Thus, **Measuring** $W^{\dagger}W$ **directly gives the flux of Hawking radiation detected**. The Klein-Gordon equation describes how a scalar field evolves in spacetime: $\sum_{\mu=0}^{3} D_{\mu} D^{\mu} f = 0$.

The function a(x) and b(x) can be interpreted as initial conditions for this equation:

$$f|_{S'} = b(x) , \dot{f}|_{S'} = -a(x)$$
 (9.10)

We can alternatively write,

$$W = \int_{S'} d\Sigma^{\mu} f \stackrel{\leftrightarrow}{\partial}_{\mu} \sigma \tag{9.11}$$

Where, $d\Sigma^{\mu}$ is the surface element associated to S'. f is the a function that represents the quantum field mode (or test function). σ is the quantum field. $\overleftrightarrow{\partial}_{\mu}$ is the antisymmetric derivative defined as : $f \overleftrightarrow{\partial}_{\mu} \sigma = f (\partial_{\mu} \sigma) - (\partial_{\mu} f) \sigma$. The quantity $f \overleftrightarrow{\partial}_{\mu} \sigma$ is a conserved current $D_{\mu} \left(f \overleftrightarrow{\partial}_{\mu} \sigma \right) = 0$. Since, this quantity is conserved, it allows us to define the same operator W on different hypersurface. Because the quantity is conserved, we can define W on different hypersurface S:

$$W = \int_{S} d\Sigma^{\mu} f \stackrel{\leftrightarrow}{\partial}_{\mu} \sigma \tag{9.12}$$

This means that instead of evaluating w on S', we can compute it on S. Physically, it means instead of looking at f on S' (where the observer is located), we solve the field equation backwards in time to find f on S. Since, f was outside the horizon on S', it must also be outside the horizon on S. To determine what f looks on S, we must solve the wave equation backwards in time. On S', f is an incoming wave of frequency ω . If we follow f backwards in time, it propagates towards the black hole and encounters a potential barrier. Some of the wave is reflected back to infinity, while some is transmitted into the near horizon region. This is crucial because it tells us that f on S contains both transmitted and reflected components.

Now we introduce the transmission and reflection coefficient in the time reversed scattering problem. T': Transmission amplitudes for a wave propagating through the potential barrier. R': Reflection amplitudes for a wave bounding back to infinity. Then equation (9.12) exhibits W as the sum of T' times a near horizon operator and R' times an operator in the Minkowski vacuum near $r = \infty$. When the observer measures $\langle W^{\dagger}W \rangle$, the terms involving R' do not contribute because operators associated with the Minkowski vacuum have zero expectation value in the vacuum. This means, terms like $|R'|^2$ vanish in the expectation value. Thus, the dominant contribution comes from T', which describe waves transmitted through the barrier. So, the relevant part of $W^{\dagger}W$ is just $|T'|^2$ times the same near horizon operator that we would have if there were no reflection from the barrier. Time-reversed symmetry means means that T' is the complex conjugate of the earlier transmission coefficient T. So, $W^{\dagger}W$ is just $|T|^2$ times what it would be if there were no potential barrier, as assumed in previous section. Therefore, as claimed, the emission rate from the black hole in a given potential wave at frequency ω is $|T(\omega)|^2$ times the thermal emission rate in the given mode at the Hawking Temperature. In the far future, quantum fields outside a black hole settle into a special state called the Unruh state. The Unruh state is Universal, meaning it does not depend on how the black hole was formed.

"Hawking radiation is not purely thermal". A naive derivation of Hawking radiation would suggest that every mode (partial wave) contributes equally, which would lead to infinite luminosity - this is clearly nonphysical. Gray body factors modify the spectrum of Hawking radiation. Instead of all modes escaping to infinity, some are partially absorbed through the Black hole. The Transmission coefficient $|T|^2$ describe the possibility that a given mode escapes to infinity. The key result is that $|T|^2$ decreases rapidly for angular momentum modes (large l), meaning only the first few partial waves contribute significantly.

If the Gray body factors did not exist, every possible mode would radiate equally, leading to an infinite amount of Hawking radiation. Instead, only the very few low energy modes escapes efficiently, giving a finite well defined luminosity. This matches the expected black hole radiation formula given earlier in the equation (8.13).

9.3 Thermodynamic Instability

This section discusses thermodynamic instability in black holes, particularly in an asymptotically flat spacetime where gravitational back reaction is ignored. There are two primary reasons for this instability:

I. Instability due to Negative Specific Heat

Imagine a black hole of mass M in equilibrium with a thermal gas at the appropriate Hawking Temperature $T = 1/8\pi GM$. In this equilibrium state, the Black Hole should ideally both absorb and emit radiation at equal rates, maintaining steady mass and temperature. Now, consider a thermal fluctuation in which the black hole emits a few more particles than it absorbs. As a result, Black Hole's Mass decreases. Since, Hawking Temperature is inversely proportional to the mass $(T \propto 1/M)$, the black hole becomes hotter as its mass decreases. Since, the black hole is now hotter than its its surrounding, it will now with very high probability emit more than it absorbs, and continue to lose mass. Thus, a runaway process occurs, eventually causing the Black Hole to fully evaporate. Conversely, if the black hole absorbs more than it emits, its mass increases. Since, the Hawking temperature decreases with increase in mass, the black hole cools down. A cooler black hole emits less radiation, allowing it to absorbs even more matter from the surroundings. This leads to uncontrolled growth of the black hole, meaning it will keep increasing in mass, without limit. Thus, any small deviation from equilibrium leads to unstable outcome, where the black hole either completely evaporates or grows without limit. This instability can formally understood by analyzing the specific heat of the black hole defined as: C = dE/dT. For a black hole, the energy is given by E = M, and temperature is $T = 1/8\pi GM$. Using these relationship, we get,

$$C = -8\pi G M^2 < 0 \tag{9.13}$$

Since, this value is negative, the black hole has a negative specific heat. A thermodynamic stability requires that the specific heat to be non-negative ($C \ge 0$). A negative specific heat means the system does not tend to return to equilibrium after a small fluctuations, confirming the instability.

II. Instability due to Gravitational Collapse of Thermal Gas

Another form instability arises from the Gravitational effects of a thermal gas. Image a region of radius R filled with a thermal gas at temperature T. The energy density of the gas is of order T^4 (due to Stefan-Boltzmann law) and its total energy inside a volume R^3 is of the order T^4 R^3 . The Schwarzschild radius of a body of that mass is of the order GT^4 R^3 .

If the size of the gas cloud R is too small, the thermal energy is concentrated enough that it will collapse into a black hole. This will happen if $R \lesssim GT^4R^3$. Simplifying, we find that the maximum allowed size of a stable thermal gas region is:

$$R \sim \frac{1}{\sqrt{GT^2}} \tag{9.14}$$

This means that if the gas cloud is larger than this critical size, it will inevitably collapse into a black hole. Thus, in an asymptotically flat spacetime it is not possible to have a stable thermal gas of arbitrary size. if a thermal gas cloud is too large or dense; its gravitational energy dominates, leading to its collapse into a black hole, thereby preventing the sustained presence of a thermal environment in such spacetimes. Now, the main question raised here is "Given the instability of a black hole in an asymptotically flat spacetime, does it even make sense to discuss equilibrium between a black hole and a thermal gas?" The answer is Yes, but only under certain conditions. The Hawking radiation is derived from QFT in a fixed spacetime background. This means that the entire discussion so far is valid only in the limit where gravitational effects are present. However, if we take the limit $G \to 0$ (which removes gravitational interactions), the instability disappear. This is actual visible in equation (9.14).

Why do Instability Disappear in the limit $G \to 0$?

If we set the temperature of the gas at the Hawking temperature of a Black hole with mass $M: T_H = 1/8\pi GM$, then the maximum region that the gas can occupy has a radius of order: $R \sim G^{3/2}M^2$. This means the thermal gas can occupy a region much larger than the Schwarzschild radius $R_s = 2GM$. For a solar mass black hole, this factor is enormous ($\sim 10^{38}$), meaning the black hole is not just embedded in a local thermal gas but in a gas that fills almost all of asymptotically flat spacetime. The fluctuations instability also turns off as $G \to 0$ to understand this, we need to decide what remains fixed as $G \to 0$. The Schwarzschild radius is related to mass by $r_s = 2GM$. Since, mass and G are linked, we cannot keep both fixed as $G \to 0$. The more natural choice is to keep r_s fixed instead of mass. Expressing the Hawking Temperature in terms of Schwarzschild radius:

$$T_H = \frac{1}{4\pi r_s}$$

In this limit $(G \to 0)$, the Hawking temperature remains fixed. The black hole mass diverges as:

$$M = \frac{r_s}{2G} \to \infty$$

If the black hole undergoes a small statistical fluctuations, its mass changes by an amount of order G. The temperature change is also of order G. This means the runaway instability described earlier (where the black hole either evaporates or grows uncontrollably) occurs only at a rate proportional to G. The timescale for significant variation in the mass of the Black Hole if of an order $1/G^2$. Since, this timescale diverges in the limit $G \to 0$, the instability effectively disappears.

How can we we achieve true Equilibrium?

Even though asymptotically flat spacetime cannot support the equilibrium state between a Black hole and a thermal gas, there is a possible way to restore stability. If we modify spacetime to include a **negative cosmological constant**, we transition from an asymptotically flat spacetime to an asymptotically Anti-de Sitter (AdS) Spacetime. This modification helps regularize the thermal gas i.e. the gas is prevented from dispersing to infinity. It becomes possible to have a stable thermal gas that fills all space. In an asymptotically Anti-di Sitter (AdS) spacetime, a sufficient large black hole has a positive Specific Heat. This prevents runaway instability, allowing for stable equilibrium between the black hole and surrounding radiation. In an Ads spacetime, equilibrium is possible because : The Black Hole's mass does not decrease uncontrollably. The surrounding radiation does not disperse into infinite space. The specific heat is positive for large black holes. However, there is an important distinction in this equilibrium: Most of the entropy is in the black hole, rather than in the radiation. The black hole is large but does not emit much radiation. This differs from a scenario in which a Black Hole along with its Radiation are in perfect thermal equilibrium with equal exchange. Instead, in AdS spacetime, the black hole is simply stable and does not evaporate.

Chapter 10

Thermodynamics of Rindler Space

10.1 Making The Cut

The Hawking effect illustrates that while the entire Universe may be in a **Pure quantum state** the portion of the Universe accessible to an outside observer (outside the event horizon) appears to be in a **Mixed state** with thermal properties. This occurs due to the loss of information hidden beyond the event horizon, leading to thermal, entropy-generating system. The thermal behavior observed in Hawking radiation also arises in a simpler setting: the Unruh effect in Minkowski space. This effect describes how an observer undergoing constant acceleration perceives the Minkowski vacuum as a thermal bath of particles. The reason for this is that such an observer only has access to part of the spacetime - specifically, a **Rindler Wedge** which leads to a situation analogous to the black hole event horizon.

What is a Rindler Wedge?

If we consider a uniformly accelerating observer, their motion prevents them from accessing the entire Minkowski space. Instead, they are confined to a Rindler Wedge, defined by:

$$x > |t|$$
 or $x < -|t|$

These inequalities define two regions: The right Rindler Wedge (x > |t|) contains all the events that can be reached by an observer undergoing constant accelerating in the positive x - direction. The left Rindler Wedge (x < -|t|) contains all events accessible to an observer accelerating in the opposite direction. The future and past regions (|t| > |x|) are causally disconnected from both wedges. **Key Idea**: A Rindler observer (someone moving with constant acceleration) cannot access the full Minkowski space. Instead, they perceive a horizon at x = |t|, analogous to black hole event horizon.

- Right Rindler Wedge (Red): The region x > |t|, representing uniformly accelerated observers.
- Left Rindler Wedge (Blue): The region x < |t|, another causally disconnected wedge.

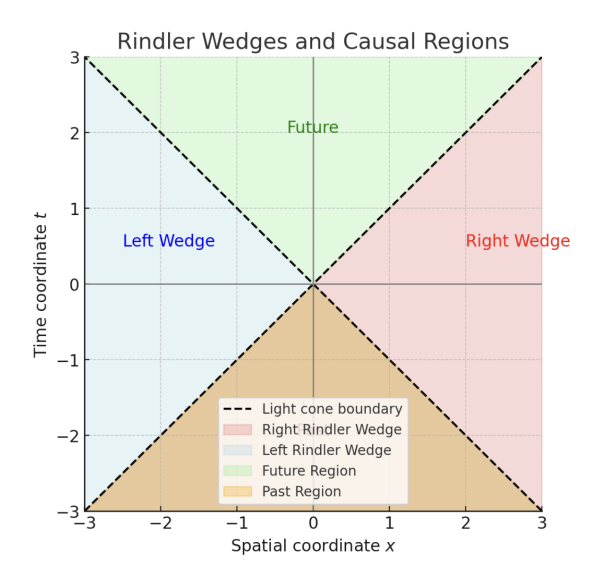


Figure 10.1: A Schematic representation of the Rindler Wedges and causal regions

- Future Region (Green): The region |t| > |x|, which is causally disconnected from both Rindler Wedges.
- Past Region (Orange): The lower triangular region, also causally disconnected from the wedges.
- Dashed Black lines: Representing the line cone boundaries $x = \pm t$.

We will begin the analysis with a Hamiltonian description on a spatial slice. A quantum state can be defined on any Cauchy hypersurface \mathcal{S} . A simple choice is t=0, the standard choice in Minkowski space. For a real scalar field ϕ , the quantum state is represented as a wave functional $\Psi(\phi(\vec{x}))$. The spatial coordinates \vec{x} are split into x (one spatial coordinates) and \vec{y} (remaining combined coordinates). The vacuum state Ω is computed using a path integral over a half-space in Euclidean time. The time coordinate is **Wick-rotated**: $t=-it_E$ to switch from Minkowski time (real time) to Euclidean time (imaginary time). The integration is performed over the field $\phi(t_E, \vec{x})$ restricted to the half-plane $t_E < 0$, keeping the boundary condition fixed at $t_E = 0$ by $\phi(\vec{x})$. This integral, as a function of $\phi(\vec{x})$, determines the vacuum wavefunction $\Omega(\phi(\vec{x}))$ (Fig 10.2 (a)). The Euclidean approach ensures that the lowest energy state (vacuum) is selected. Thus, by restricting to the half-space $t_E < 0$, the path integral constructs the ground state (vacuum) by filtering out excited states. The result is well-defined wave functional $\Omega(\phi(\vec{x}))$, evaluated at $t_E = 0$.

In quantum field theory (QFT), the vacuum state Ω is the lowest energy state of the system. The **projection operator** onto this state is given by : $\rho = \Omega\Omega$. This operator can also be interpreted as the **density matrix** associated with the pure state Ω . The key idea here is that both Ω and Ω can be represented using the path integral in Euclidean space. Let's explore this is more detail. We know from the earlier discussion that to construct the vacuum state, we use a Euclidean path integral over a half-space in imaginary time t_E , obtained via Wick rotation $t = -it_E$. The **ket** Ω is constructed using a Euclidean path integral

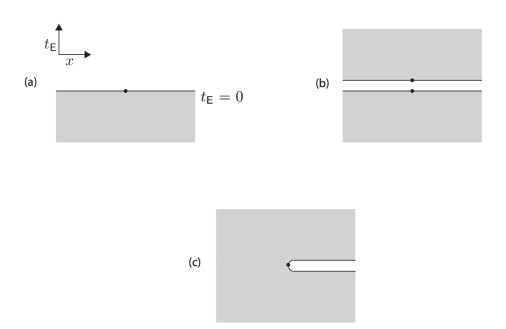


Figure 10.2: (a) A Euclidean path integral on the half-space $t_E \leq 0$ that prepares the vacuum state Ω . (b) To prepare the pure state density matrix Ω Ω associated to the vacuum, we prepare the ket Ω as just described by a path integral on the half-plane $t_E \leq 0$, and we use a similar path integral on the half-space $t_E \geq 0$ to prepare the bra Ω . Two copies of the x axis, appearing respectively as the boundary of the lower and upper half-planes, have been separated for visibility. (c) To construct the reduced density matrix ρ of the half-line x > 0, we "trace out" the quantum fields in the region x < 0. In path integrals, this is accomplished by gluing together the two copies of the negative x axis. The result is a path integral on Euclidean space with a cut along $t_E = 0$, $t_E > 0$. The density matrix $t_E > 0$ is determined by the field values just above and below the cut.

over the **lower half-space**, where $t_E \leq 0$. The **bra** Ω is constructed using a similar Euclidean path integral over the **upper half-space**, where $t_E \geq 0$ (fig 10.2 (b)). Each of these integral is performed while keeping the boundary values of the field at $t_E = 0$. The result is that : $\rho = \Omega\Omega$ can be obtained by performing the Euclidean path integral over the entire Euclidean space, gluing together the upper and lower half-spaces. We can thus view the pure state density matrix ρ as a function of pairs of boundary values:

$$\rho(\phi; \phi') = \Omega(\phi)\Omega(\phi') \tag{10.1}$$

Here, ϕ is the boundary value of $\phi(t_E, \vec{x})$ on the upper boundary of the lower half plane, and ϕ' is the boundary value of $\phi(t_E, \vec{x})$ on the lower boundary of the upper half plane. To introduce a subsystem, we divide the t = 0 surface S into the partial Cauchy surfaces S_r with $x \geq 0$ (Right region) and S_ℓ with $x \leq 0$ (Left region). Corresponding to this, we decompose the field $\phi(\vec{x})$ as a pair (ϕ_ℓ, ϕ_r) where ϕ_ℓ is the restriction of ϕ to the right region S_r . We view the ground state wavefunction as a function $\Omega(\phi_\ell, \phi_r)$. We introduce a Hilbert space \mathcal{H}_r of functions of ϕ_r and a Hilbert space \mathcal{H}_ℓ of functions ϕ_ℓ . The formally $\mathcal{H} = \mathcal{H}_\ell \otimes \mathcal{H}_r$ and in particular $\Omega \in \mathcal{H}_\ell \otimes \mathcal{H}_r$.

We would like to construct the reduced density matrix of the vacuum state Ω for an observer who can measure ϕ_r only and not ϕ_ℓ . for this, we first write equation (10.1) in more detail, with $\phi = (\phi_\ell, \phi_r)$ and $\phi' = (\phi'_\ell, \phi'_r)$:

$$\rho(\phi_{\ell}, \phi_r; \phi_{\ell}', \phi_r') = \Omega(\phi_{\ell}, \phi_r) \Omega(\phi_{\ell}', \phi_r')$$
(10.2)

An observer in the right region S_r has access only to measurements of ϕ_r and not ϕ_ℓ . To obtain the reduced density matrix ρ_r for such an observer, we must trace

out (integrate over) the unobserved variables ϕ_{ℓ} . This means setting $\phi_{\ell} = \phi'_{\ell}$ and integrating over all possible values of ϕ_{ℓ} . This gives the density matrix $\rho_r(\phi_r; \phi'_r)$ appropriate for measurements of ϕ_r :

$$\rho_r(\phi_r; \phi_r') = \int D\phi_\ell \,\Omega(\phi_\ell, \phi_r) \Omega(\phi_\ell', \phi_r') \tag{10.3}$$

Here, $D\phi_{\ell}$ plays the role of summing over all hidden possibilities of the left region. This integral sums over all field configurations in the left region, effectively forgetting the unobserved degrees of freedom.

How do we represent ρ_r by a path integral?

Initially, we start with a pure density matrix $\rho = \Omega\Omega$ which can be expressed as a path integral over the Euclidean space \mathbb{R}^4 , but with a cut on the hypersurface \mathcal{S} defined by Euclidean time $t_E = 0$, and thus with separate boundary values ϕ , ϕ' below and above the cut. Now, to obtain the reduced density matrix ρ_r (10.3) for a subregion S_r , we must trace out the degrees of freedom in the complementary region \mathcal{S}_{ℓ} . Instead of treating the field values separately above and below the cut in \mathcal{S}_{ℓ} , we impose the condition that they are equal. This means we glue the upper and lower half-spaces together along \mathcal{S}_{ℓ} , effectively removing the cut in that region. After identifying the field values in \mathcal{S}_{ℓ} , we integrate over these values. This procedure corresponds to performing the trace over \mathcal{S}_{ℓ} , effectively removing those degrees of freedom from the description. We end up with a path integral now that (fig 10.2 (c)) covers all of \mathbb{R}^4 except for a remaining cut in \mathcal{S}_r . The boundary values below and above the cut are ϕ_r and ϕ_r' and a path integral on \mathbb{R}^4 with this cut and with fixed boundary values above and below the cut computes the matrix elements $\rho_r(\phi_\ell; \phi'_\ell)$ of the density matrix ρ_r of \mathcal{S}_r . Similarly, a density matrix appropriate for measurements of ϕ_{ℓ} only is obtained by setting $\phi_r = \phi'_r$ in ρ and integrating over ϕ_r :

$$\rho_{\ell}(\phi_{\ell}; \phi_{\ell}') = \int D\phi_r \,\Omega(\phi_{\ell}, \phi_r) \Omega(\phi_{\ell}', \phi_r') \tag{10.4}$$

It can be represented by a path integral on \mathbb{R}^4 with a cut along $t_E = 0$, x < 0.

The relations to all this Rindler space is as follows: In Lorentzian spacetime, the domain of dependence of a partial Cauchy surface \mathcal{S}_r Rindler Wedge (\mathcal{R}_r) . Mathematically, the right Rindler Wedge is defined by the condition: x > |t| (Fig (10.3)). This means that any event in R_r is completely determined by initial data on \mathcal{S}_r , as causal influences cannot come from outside this region. Regardless of the specific quantum field theory being considered, the equations of motion for fields in \mathcal{R}_r are fully determined by their initial conditions on \mathcal{S}_r . This follows from the hyperbolic nature of field equations (such as the wave equations), which propagate information causally. Any measurements in \mathcal{R}_r corresponds to measuring the field ϕ_r in that region. The density matrix ρ_r provides a covariant description of these measurements in \mathcal{R}_r . The opposite wedge, called the left-Rindler Wedge (\mathcal{R}_ℓ) is defined by: x < -|t|. Measurements in this region corresponds to another field ϕ_ℓ and the appropriate density matrix for this region ρ_ℓ . This means that an observer in \mathcal{R}_ℓ would describe their system using ρ_ℓ , independent of what happens in \mathcal{R}_r .

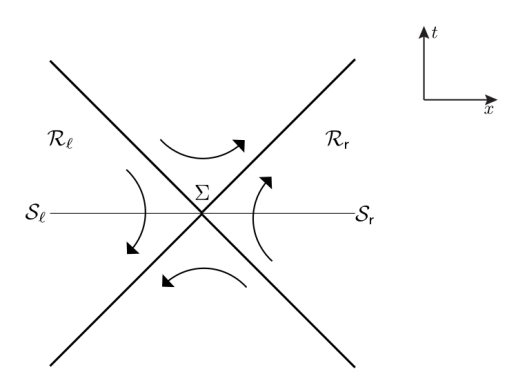


Figure 10.3: In Minkowski space, the left and right Rindler wedges \mathcal{R}_{ℓ} and \mathcal{R}_{∇} are defined as the domains of dependence of the partial Cauchy hypersurfaces \mathcal{S}_{ℓ} and \mathcal{S}_{∇} . The diagonal lines mark the boundaries of \mathcal{R}_{ℓ} and \mathcal{R}_{∇} ; they are the past and future horizons of an observer who remains forever in \mathcal{R}_{ℓ} or \mathcal{R}_{∇} and limit the portion of spacetime that the observer can see or influence. All past and future horizons meet at the bifurcation surface Σ , which also marks the common boundary of \mathcal{S}_{ℓ} and \mathcal{S}_{∇} . The arrows indicate the action of the Lorentz boost generator K, which is future-directed timelike in \mathcal{R}_{∇} , past-directed timelike in \mathcal{R}_{ℓ} , and spacelike elsewhere.

Following are few important facts about the geometry of Rindler space. Firstly, in order to remains forever in the right Rindler wedge (\mathcal{R}_r) , an observer must accelerate indefinitely, in the future and also in the past. This means that an observer in \mathcal{R}_r never crosses the Rindler horizon and always remains within their casually connected region, as in equation (10.10) below, (that suggests that it will later be linked to the Unruh effect) (The phenomenon where an accelerating observer perceives a thermal bath of particles). The visible region for an observer in \mathcal{R}_r is bounded by the past and future Rindler horizons, represented by a diagonal line in Fig (10.3). Similarly, an observer in the left left Rindler Wedge (\mathcal{R}_{ℓ}) experiences their own past and future horizons. The horizons of both Wedges intersect at a co-dimension two surface called bifurcation surface Σ . This surface is also referred to as the entangling surface, marking the boundary between the partial Cauchy surface S_r and S_ℓ . Studying Rindler Space helps us understand black hole Thermodynamics and horizon physics. The right and left Rindler Wedges (\mathcal{R}_r) and (\mathcal{R}_ℓ) are invariant under Lorentz boosts in the x-t plane. This means that the physics in these Wedges remains unchanged under boosts transformation. This symmetry has played no role up to this point, but now that will change.

10.2 Boosts and The Unruh Effects

The density matrix ρ_r can be understood in another way by emphasizing the rotational symmetry of the $x-t_E$ plane. Actually, it is convenient to first relate a rotation in Euclidean signature to a boosts in Lorentz signature.

In Lorentz Signature, the generators of a boost of the x-t plane is :

$$K = \int_{S} dx \, d\vec{y} \, x \, T_{00}(x, \vec{y}) \tag{10.5}$$

Where T_{00} represents the energy density. The boost generator can be expressed as:

$$K = K_r - K_\ell \tag{10.6}$$

With,

$$K_{r} = \int_{S_{r}} dx \, d\vec{y} \, x \, T_{00}(x, \vec{y})$$

$$K_{\ell} = \int_{S_{\ell}} dx \, d\vec{y} \, |x| \, T_{00}(x, \vec{y}),$$
(10.7)

Where K_r generates a Lorentz boost of ϕ_r and K_ℓ generates a Lorentz boost of ϕ_ℓ . K_r generates a Lorentz boost of the right Rindler Wedge \mathcal{R}_r and commutes with operators in the spacelike separated Wedge \mathcal{R}_ℓ and commutes with operators in \mathcal{R}_r . A minus sign was included in equation (10.6) so that K_r and K_ℓ each boost the corresponding Rindler Wedge forward in time. There is an additive ambiguity in the definition of T_{00} , and we assume this has been fixed so that the Vacuum energy density vanishes, otherwise the integrals defining K_ℓ and K_r diverges. The operator $e^{-i\eta K_r}$, with real η , acts on ϕ_r by a Lorentz boost with boost parameter η . If we set $\eta = -i\theta$, the Lorentz boost turns into a rotation and we get the operator $\exp(-\theta K_r)$ that in Euclidean signature rotates the $x-t_E$ plane by an angle θ . In terms of path integrals, this means that to compute a matrix element of $\exp(-\theta K_r)$ acting on θ_r , we need to perform a path integral on a wedge of opening angle θ . If we simply set $\theta = 2\pi$, the wedge opening angle θ becomes the cut plane of Fig 10.(c). Therefore, we get a formula for the density matrix ρ_r :

$$\rho_r = \exp(-2\pi K_r) \tag{10.8}$$

Similarly,

$$\rho_{\ell} = \exp(-2\pi K_{\ell}) \tag{10.9}$$

The trace condition $\text{Tr}\rho = 1$ is verified using a path integral over the entire plane. Since the energy-momentum tensor is renormalized to have a vanishing vacuum expectation value, the path integral is properly normalized. The interpretation of K_r as a Hamiltonian of the right Rindler wedge \mathcal{R}_r implies that the density matrix ρ_r is **thermal** at an Inverse temperature 2π . This leads to the **Unruh Effect** - An observer undergoing constant acceleration in Minkowski space perceives thermal radiation.

An illustration of a trajectory under uniform acceleration is:

$$t = L \sinh \frac{\tau}{L}, x = L \cosh \frac{\tau}{L}, \vec{y} = 0$$
 (10.10)

Where τ is the proper time of the observer, and 1/L is the magnitude of the acceleration. Any uniformly accelerated orbit in Minkowski space has this form for some choice of Rindler Wedge and some L. The Lorentz boost generator K_r acts on this orbit as $L\frac{d}{d\tau}$, So the observer could interpret K_r as L times the natural Hamiltonian. Of course the definition (10.7) for K_r shows that for observations near x = L, K_r can be approximate as LH where $H = \int_{S_r} dx \, d\vec{y} \, T_{00}$ is the Hamiltonian acting on the Right Rindler Wedge.

A quick way to become convinced that the observations of such an observer

will be thermal is to continue the orbit to Euclidean signature. In Euclidean signature, with $t = it_E$, $\tau = i\tau_E$, the orbit becomes:

$$t_E = L \sinh \frac{\tau_E}{L}, \quad x = L \cosh \frac{\tau_E}{L}, \quad \vec{y} = 0$$
 (10.11)

This orbit is periodic in τ_E with period $2\pi L$, suggesting that the observer will see thermal correlations at temperature $1/2\pi L$. The periodicity measured along the Lorentz signature orbit (5.10) implies the presence of thermal effects, interpreted using the **Kubo-Martin-Schwinger (KMS) condition**, which characterizes thermal equilibrium in QFT. The temperature associated with this observer's point of view, K_r is interpreted as noted earlier as LH, with H the relevant Hamiltonian, So the formula (10.8) becomes $\rho_r = \exp(-2\pi LH)$, leading naturally to thermal correlations at temperature $1/2\pi L$. Thus, a uniformly accelerated observer or one restricted to a Rindler Wedge perceives the Minkowski Vacuum as a thermal state. The temperature is linked to the acceleration and is inversely proportional to the distance from the edge of the Rindler Wedge at the bifurcation surface Σ : x = t = 0, so this temperature diverges near bifurcation surface (Σ) and vanishes at infinity. The conclusion is validated by the KMS condition, which is a criterion for thermal equilibrium in QFT.

After developing The Euclidean framework for understanding black hole thermodynamics in section 11; we will be able to give a precisely parallel derivation of the thermal nature of the black hole spacetime. The main difference is that, for black holes, the temperature does not vanish at infinity but is instead equal to the **Hawking Temperature**. This is crucial result, as it shows that black hole spacetime have an inherent thermal nature. A noteworthy fact about the derivation for Rindler space, and the upcoming black hole derivation is that it does not depend on the specific Quantum field Theory under consideration. It implies even if there are arbitrary non-gravitational forces. The assumption of a single scalar field ϕ is made only for convenience and does not restrict the generality of the result.

The earlier discussion on black hole evaporation (in Chapter 8) ignored nongravitational forces. However, the thermal nature of the Rindler and black hole horizons is derived with such assumptions making it more robust.

10.3 The Thermofield Double

For some Hilbert space \mathcal{H} , let $\rho: \mathcal{H} \to \mathcal{H}$ be a density matrix. In general a density matrix is simply a positive (or non-negative) matrix with trace 1. **Purification** is a technique used in quantum mechanics to represent a mixed state as part of a larger pure state in an extended Hilbert space. Given a mixed state ρ in Hilbert space \mathcal{H} , We introduce an auxiliary Hilbert space \mathcal{H}' and construct a pure state Ψ in the combined system (Double space) $\mathcal{H} \otimes \mathcal{H}'$, such that:

$$\rho = \text{Tr}_{\mathcal{H}'} \Psi \Psi \tag{10.12}$$

Where $\Psi\Psi$ is the pure density matrix. Equation (10.12) implies that the original matrix state ρ is obtained by taking the partial trace over \mathcal{H}' .

Every density matrix has a canonical purification, i.e ut can be represented

as a part of pure state in an enlarged Hilbert space. For a vector space \mathcal{K} , if $\mathcal{V}: \mathcal{K} \to \mathcal{K}$ is a linear transformation, it can be expressed in a basis as:

$$\mathcal{V} = \sum_{i,j} v_{ij} \, ij \tag{10.13}$$

Given this, we can associate to $\mathcal V$ a vector $\Psi_{\mathcal V}$ in a doubled Hilbert Space $\mathcal K\otimes\mathcal K'$:

$$\Psi_{\mathcal{V}} = \sum_{i,j} v_{ij} \, i \otimes j \tag{10.14}$$

Where \mathcal{K}' is the complex Hilbert Space of \mathcal{K} , meaning that to each bra j of \mathcal{K} there is canonically associated a ket $j' \in \mathcal{K}'$. Tracing out \mathcal{K}' from the pure density matrix $\Psi_{\mathcal{V}}\Psi_{\mathcal{V}}$, we get :

$$\mathcal{V}\mathcal{V}^{\dagger} = \text{Tr}_{\mathcal{K}'}\Psi_{\mathcal{V}}\Psi_{\mathcal{V}} \tag{10.15}$$

Thus, if $\operatorname{Tr} \mathcal{V} \mathcal{V}^{\dagger} = 1$, so that $\mathcal{V} \mathcal{V}^{\dagger}$ is a density matrix, then $\Psi_{\mathcal{V}}$ is a purification of this density matrix. This enables us to define the canonical purification of a density matrix. If ρ is any density, then it is the square of $\rho^{1/2}$. So $\Psi_{\rho^{1/2}} \in \mathcal{H} \otimes \mathcal{H}'$ is a purification of ρ , is called the **Canonical Purification**.

For an important example, consider the thermal density matrix of a system with Hilbert space \mathcal{H} and Hamiltonian H at inverse temperature β :

$$\rho = \frac{1}{Z} \sum_{i} e^{-\beta E_i} ii \tag{10.16}$$

Where i are the energy Eigenstates of the Hamiltonian H with corresponding energy E_i . $Z = \sum_i e^{-\beta E_i}$ is the partition function which ensures that ρ has trace 1. $\beta = 1/T$ is the inverse temperature. The density matrix describes a thermal ensemble, meaning that the system has a probability distribution over energy Eigenstates. This a mixed state since it represents a statistical mixture of energy Eigenstates rather than a pure quantum state. The Canonical purification of a thermal density matrix is then the state in $\mathcal{H} \otimes \mathcal{H}'$ associated to $\rho^{1/2}$:

$$\Psi_{\text{TFD}} = \frac{1}{Z} \sum_{i} e^{-\beta E_i} i \otimes i'$$
 (10.17)

This state is also called the **Thermofield Double**. The Thermofield Double (TFD) state is a pure entangled state in the double Hilbert space $\mathcal{H} \otimes \mathcal{H}'$. The state i' belong to an auxiliary space \mathcal{H}' , which is often taken as the complex conjugate Hilbert space of \mathcal{H} . The TFD state is very important in holography, black hole physics, and quantum information. It describe an entangled state of two identical copies of the system at the same temperature β^{-1} . In Holography, it is often used to model two-sided black holes in Ads—CFT. \mathcal{H}' is typically considered as a complex conjugate of \mathcal{H} . However, if the system has an anti-linear time reversal symmetry whose square is 1, the distinction between \mathcal{H} and \mathcal{H}' is not important.

Every Quantum Field Theory (QFT), has a **CRT** symmetry which a combination of **Charge Conjugation** (C) which exchange particles with anti-particles,

spatial **Reflection** (**R**) which reflects space and **Time Reversal** (**T**) that reverses the direction of time. This symmetry exchange left and right Rindler Wedges (regions in Minkowski space separated by event horizons) and swaps the Hilbert Space \mathcal{H}_{ℓ} with \mathcal{H}'_r (Because CRT is anti-linear, it exchanges \mathcal{H}_{ℓ} with \mathcal{H}'_r , not \mathcal{H}_r). So instead of $\mathcal{H}_r \otimes \mathcal{H}'_{\ell}$, the vacuum vector Ω can be viewed as a vector in $\mathcal{H}_r \otimes \mathcal{H}'_r$, the expected home of the Thermofield double state.

We will work out the Thermofield double state for a bosonic or fermionic harmonic oscillator. First we will consider an ordinary bosonic harmonic oscillator with creation and annihilation operators a^{\dagger} and a satisfying $[a,a^{\dagger}]=1$ and Hamiltonian $H=\omega\,a^{\dagger}a$. The thermal density matrix at inverse temperature β is :

$$\rho = \frac{1}{Z} \sum_{n=0}^{\infty} e^{-n\beta\omega} nn \tag{10.18}$$

Where n is the $n^{\rm th}$ excited state of the harmonic oscillator. The Thermofield double state for this system is :

$$\Psi_{\text{TFD}} = \frac{1}{Z} \sum_{n=0}^{\infty} e^{-n\beta\omega/2} \, n \otimes n' \tag{10.19}$$

Here, n' is the n^{th} excited state of an identical second harmonic oscillator with creation and annihilation operators ${a'}^{\dagger}$, a'. Note: The Thermofield double state is a purification of the thermal density matrix, meaning that if we trace out one system, we recover the original mixed thermal state. Now using $a^{\dagger} n = \sqrt{n+1} \, n+1$, etc., we find:

$$(a^{\dagger} - e^{\beta\omega/2} a') \Psi_{\text{TFD}} = (a - e^{\beta\omega/2} a'^{\dagger}) \Psi_{\text{TFD}} = 0$$
 (10.20)

These equations uniquely define the Thermofield double state (Ψ_{TFD}) up to a scalar multiple. For Fermionic Oscillators, these formulas contains an extra minus sign-associated to fermi statistics. We consider fermionic creation and annihilation operators c^{\dagger} , c obey anti-commutation relation $\{c, c^{\dagger}\} = 1$, acting on a two-dimensional Hilbert space 0 and another state $1 = c^{\dagger}0$. Assuming a Hamiltonian $H = \omega c^{\dagger}c$, the thermal density matrix is:

 $\rho = \frac{1}{Z} \left(00 + e^{-\beta \omega} 11\right)$. To construct the Thermofield double state, we introduce a second identical fermionic oscillator with creation and annihilation operators \tilde{c}^{\dagger} , \tilde{c} that anti-commute with c,c^{\dagger} . These operators can be represented in a four-dimensional Hilbert space with a state 0,0 annihilated by both c and \tilde{c} and additional states $1,0=\tilde{c}0,0,0,1=\tilde{c}^{\dagger}0,0,1,1=c^{\dagger}\tilde{c}^{\dagger}0,0$. The Thermofield double state is then:

$$\Psi_{\text{TFD}} = \frac{1}{Z^{1/2}} \left(0, 0 + e^{-\beta \omega/2} 1, 1 \right) \tag{10.21}$$

and satisfies,

$$(c - e^{-\beta\omega/2} \tilde{c}^{\dagger}) \Psi_{TFD} = 0$$

$$(c^{\dagger} + e^{\beta\omega/2} \tilde{c}) \Psi_{TFD} = 0.$$
(10.22)

10.4 Another View of The Thermofield Double

The Vacuum state Ω of Minkowski space can be interpreted as a Thermofield Double state of two Rindler Wedges. This idea is limited to Free Field Theory but still provides an insightful way of understanding the Thermofield double state. Instead of working in full Minkowski space, we will only consider the case of a chiral free fermion in two dimensional space time. The idea is to show that the Vacuum state obeys conditions to equations (10.22). Consider two-dimensional Minkowski space with metric $ds^2 = -dt^2 + dx^2 = -dudv$, where $v = \frac{1}{\sqrt{2}}(t+x)$, and $u = \frac{1}{\sqrt{2}}(t-x)$ are null coordinates. The operator P generates translations in v and is positive definite, meaning it annihilates only the Vacuum. Mathematically this means P satisfies:

$$[P, O] = -i\frac{d}{dv}\mathcal{O} \tag{10.23}$$

For any operator \mathcal{O} . This equation tells us how the vacuum state behaves under translations in v.

Next, we introduce a chiral free fermion field $\lambda(v)$ that satisfies the anti-commutation relation :

$$\{\lambda(v), \lambda(v')\} = \delta(v - v') \tag{10.24}$$

We define the Fourier modes of the field $\Lambda_{\omega} = \int_{-\infty}^{\infty} dv e^{-i\omega v} \lambda(v)$, this represents a mode decomposition of the fermion field into different frequency components ω . These modes satisfy the anti-commutation relation:

$$\{\Lambda_{\omega}, \Lambda_{\omega'}\} = 2\pi\delta(\omega + \omega') \tag{10.25}$$

This equation tells us that different frequency modes interact in a specific way, governed by the Dirac Delta function. Next, we look at the action of the momentum operator P on these Fourier modes :

$$[P, \Lambda_{\omega}] = \omega \Lambda_{\omega} \tag{10.26}$$

So operators Λ_{ω} are creation operators for $\omega > 0$ and annihilation operators for $\omega < 0$. To be more precise, these operator are creation operators (add quanta / particle to the vacuum state) to the Minkowski vacuum or equivalently they are raising and lowering operators with respect to P. The annihilation operators annihilate the vacuum:

$$\Lambda_{\omega} \Omega = 0, \ \omega < 0 \tag{10.27}$$

More generally, any operator:

$$\Lambda_f' = \int_{-\infty}^{\infty} dv \, f(v) \lambda(v) \tag{10.28}$$

will annihilate the vacuum if the function f(v) has certain mathematical properties. specifically it must be Holomorphic (complex differentiable) and bounded in the upper half of the complex plane. Indeed, a square-integrable function f(v) is holomorphic and bounded in the upper plane if and only if:

$$f(v) = \int_{-\infty}^{0} d\omega e^{-i\omega v} g(\omega)$$
 (10.29)

Where $g(\omega)$ is some integrable function. The restriction $\omega < 0$ is crucial. It means that the function f(v) does not contain positive frequency components $(\omega > 0)$. The reason for this is that terms like $e^{-i\omega v}$ with $\omega > 0$ grow exponentially in the upper half v - plane, which would violet the Holomorphic condition. Since, f(v) only contains negative-frequency components, the corresponding operator Λ'_f is a linear combination of annihilation operators and thus annihilates the vacuum. Now lets discuss the perspective of an operator in the right Rindler wedge \mathcal{R}_{∇} , defined by the conditions: x > |t| or v > 0, u < 0. This region corresponds the part of the Minkowski space accessible to an uniformly accelerated observer. Instead of using global Minkowski coordinates, such an observer naturally describe physics in terms of Rindler coordinates, where time evolution is generated by a different Killing vector field in the u-v plane is: $\|=v\partial_v-u\partial_u$. This vector generates Lorentz boosts, which acts as translations in Rindler time. It is future-directed and timelike inside the Wedge \mathcal{R}_{∇} , meaning it behaves like a Hamiltonian generating time evolution for an observer in \mathcal{R}_{∇} . Thus, the observer perceive vacuum as evolving under this generator, leading to thermal state in the Rindler frame. A Hermitian conserved charge K is associated with the killing vector k, and plays the role of Hamiltonian in the Rindler Wedge. (K Rindler Hamiltonian).

For a chiral fermion field $\lambda(v)$, the action of k reduces to : $k \lambda(v) = v \partial_v \lambda(v)$. Since K is the generator of the translations in Rindler time, its commutator with $\lambda(v)$ follows the equation : $[K, \lambda(v)] = -i(v d_v + \frac{1}{2}) \lambda(v)$ (Where the +1/2) reflects the fact that λ has a spin 1/2). The observer in \mathcal{R}_{∇} only measures $\lambda(v)$ for v > 0. To analyze these modes, we define a new set of operators :

$$U_{\omega} = \int_0^{\infty} dv \, v^{-i\omega - \frac{1}{2}} \, \lambda(v) \tag{10.30}$$

These operators satisfy the commutator relation:

$$[K, U_{\omega}] = \omega U_{\omega} \tag{10.31}$$

Hence, with respect to K, U_{ω} is a raising operators, or a creation operator, if $\omega > 0$ and a lowering operator or an annihilation operator, if $\omega < 0$. Moreover,

$$U_{\omega}^{\dagger} = U_{-\omega} \tag{10.32}$$

This means that the creation and annihilation operators are related in a simple way: the Hermitian conjugate of a creation operator at frequency ω is an annihilation operator at frequency $-\omega$. While U_{ω} was shown to be a raising or lowering operator with respect to the Rindler Hamiltonian K, it does not annihilate the Minkowski space vacuum state Ω . The reason is related to the holomorphic structure of the function:

$$f(v) = \begin{cases} v^{-i\omega - \frac{1}{2}} & \text{if } v > 0\\ 0 & \text{if } v < 0 \end{cases}$$
 (10.33)

This function is not holomorphic in the upper half-plane of v, meaning it does not smoothly extend over the entire complex plane. To get an annihilation operator for the Minkowski vacuum that is equivalent to U_{ω} , $\omega < 0$ for observations in the

right Rindler Wedge, we need to modify f(v) to be non-zero for v < 0 in such a way that f(v) becomes holomorphic and bounded in the upper half plane. A function that coincides with f(v) for v > 0 and is bounded in the upper half v - plane is $(v + i\epsilon)^{-i\omega - \frac{1}{2}}$ where ϵ is an infinitesimal positive quantity $(\epsilon \to 0^+, \epsilon)$ ensuring smoothness in the upper half plane. The boundedness in the upper half plane holds for either sign of ω . Hence, for all ω ,

$$V_{\omega} = \int_{-\infty}^{\infty} dv \, (v + i\epsilon)^{-i\omega - \frac{1}{2}} \, \lambda(\omega)$$
 (10.34)

This operator V_{ω} properly annihilates the Minkowski vacuum Ω and serves as the correct annihilation operator. We now evaluate the limit: $\lim_{\epsilon \to 0^+} (v + i\epsilon)^{-i\omega - \frac{1}{2}}$. This function behaves differently for positive and negative values of v:

$$\lim_{\epsilon \to 0^+} (v + i\epsilon)^{-i\omega - \frac{1}{2}} = \begin{cases} v^{-i\omega - \frac{1}{2}} & \text{if } v > 0\\ -ie^{\pi\omega} (\overline{v})^{-i\omega - \frac{1}{2}} & \text{if } v < 0, \end{cases}$$
(10.35)

Where $\overline{v} = -v$. Equation (10.35) introduces an important exponential factor $e^{\pi\omega}$ for negative v, which will play a crucial role in understanding the thermality of the vacuum state. To systematically describe the contributions from both positive and negative of v, we define a new operator:

$$\tilde{U}_{\omega} = \begin{cases}
i \int_{0}^{\infty} d\,\overline{v}\,\overline{v}^{i\omega - \frac{1}{2}} \,\lambda(\overline{v}) & \text{if } \omega < 0 \\
-i \int_{0}^{\infty} d\,\overline{v}\,\overline{v}^{i\omega - \frac{1}{2}} \,\lambda(\overline{v}) & \text{if } \omega > 0
\end{cases}$$
(10.36)

Here, $\overline{v} = -v$ represents the negative values of v, which naturally corresponds to the left Rindler Wedge \mathcal{R}_{ℓ} . Since, the left Rindler Wedge is a mirror reflection of the right Rindler Wedge, the sign reversal ensures that \tilde{U}_{ω} behaves like a creation operator for $\omega > 0$ and annihilation operator for $\omega < 0$ in \mathcal{R}_{ℓ} . This leads to fundamental identity $\tilde{U}_{\omega} = \tilde{U}_{-\omega}$ in parallel with equation (10.32). Relative to (10.34), We have reversal the sign of ω in the exponent. The reason is that v increases towards the future in \mathcal{R}_r , but \bar{v} increases towards the past in \mathcal{R}_{ℓ} . Hence, the sign reversal is needed if we want \tilde{U}_{ω} to look in \mathcal{R}_{ℓ} like a creation operator if $\omega > 0$ and an annihilation operator if $\omega < 0$. Using these definitions, We express V_{ω} as:

$$V_{\omega} = \begin{cases} U_{\omega} - e^{\pi\omega} \widetilde{U}_{-\omega} = U_{\omega} - e^{\pi\omega} \widetilde{U}_{\omega}^{\dagger} & \omega < 0 \\ U_{\omega} + e^{\pi\omega} \widetilde{U}_{-\omega} = U_{\omega} + e^{\pi\omega} \widetilde{U}_{\omega}^{\dagger} & \omega > 0. \end{cases}$$
(10.37)

This expression demonstrates that the Minkowski vacuum is a superposition of Right Rindler vacuum states, with entanglement between the left and right Wedges. Thus, the key takeaway from this analysis is that Minkowski vacuum state Ω is a Thermofield Double state with respect to the Right Rindler Wedge \mathcal{R}_r , meaning: The vacuum state contains entanglement between the left and right Rindler Wedges. The Right Rindler observer perceives the Minkowski vacuum as a Thermal State with an inverse temperature $\beta = 2\pi$. The exponential factor $e^{i\pi}$ appearing in the mode decomposition is a Signature of Thermal Radiation, leading to the Unruh Effect, Where an accelerating observer experiences a thermal bath of particles at temperature: $T = 1/2\pi$. The

statement that $V_{\omega} \Omega = 0$ for $\omega < 0$ matches with the first condition n equation (10.22), and the statement that $V_{\omega} \Omega = 0$ for $\omega > 0$ matches the second one. The key result is that the Vacuum state Ω can be rewritten as a Thermofield double state of two entangled subsystem (the two Rindler Wedges). In context of Black holes this tells us that The Hawking Radiation is entangled with the Black hole interior in a structure that resembles a Thermofield Double State.

Chapter 11

Conclusions and Scope for Future Work

This project has covered the key developments in black hole theory, starting with their historical development and radiative properties. The analysis explores the Schwarzschild metric along with multiple coordinate systems crucial for interpreting spherically symmetric black holes. It delves into black hole perturbations using weak-field approximations and examines solutions involving scalar fields. Additionally, it addresses quantum particle generation in the vicinity of black holes, highlighting the importance of mode decomposition and basis selection as foundational steps in deriving Hawking radiation. These discussions provide a foundation for further exploration of black hole thermodynamics and quantum field theory in curved spacetime. It also discusses key developments in black hole thermodynamics, Starting from the notion of black hole entropy and its linkage to the generalized 2nd law of thermodynamics, the analysis proceeds to explore black hole evaporation using a range of Penrose diagram representations and introduces relationships describing the position of a distant observer detecting Hawking radiation, as well as the rate at which this radiation is observed. Additionally, we establish how the Hawking temperature relates to the Schwarzschild radius and derive an expression for Black hole evaporation. Moreover, It's explores Gray body factors, deriving several equations for the potential barrier around the Black hole. This barrier dictates the proportion of Hawking radiation that escapes to infinity—where a distant observer can detect it—while the remaining radiation is reflected back into the black hole. Lastly, the final chapter focuses on a detailed study of the thermodynamics of Rindler space and how it helps us to understand black hole thermodynamics by focusing on the key quantum effects, without needing full gravity...

Appendices

Appendix A

Regge-Wheeler equation

$$\left[\frac{\partial^{2}}{\partial r_{*}^{2}} - \frac{\partial^{2}}{\partial t^{2}} - V_{\ell}(r)\right] \hat{u}_{\ell}(r,\omega) e^{-i\omega t} = 0$$

$$\left[\frac{\partial^{2} \hat{u}_{\ell}(r,\omega) e^{-i\omega t}}{\partial r_{*}^{2}} - \frac{\partial^{2} \hat{u}_{\ell}(r,\omega) e^{-i\omega t}}{\partial t^{2}} - V_{\ell}(r) \hat{u}_{\ell}(r,\omega) e^{-i\omega t}\right] = 0$$

$$\left[\frac{\partial^{2} \hat{u}_{\ell}(r,\omega) e^{-i\omega t}}{\partial r_{*}^{2}} - \left(-\omega^{2} e^{-i\omega t} \hat{u}_{\ell}(r,\omega)\right) - V_{\ell}(r) \hat{u}_{\ell}(r,\omega) e^{-i\omega t}\right] = 0$$

$$\left[\frac{\partial^{2} \hat{u}_{\ell}(r,\omega) e^{-i\omega t}}{\partial r_{*}^{2}} + \left(\omega^{2} e^{-i\omega t} \hat{u}_{\ell}(r,\omega)\right) - V_{\ell}(r) \hat{u}_{\ell}(r,\omega) e^{-i\omega t}\right] = 0$$

$$\left[\frac{\partial^{2} \hat{u}_{\ell}(r,\omega) e^{-i\omega t}}{\partial r_{*}^{2}} + \left(\omega^{2} e^{-i\omega t} \hat{u}_{\ell}(r,\omega)\right) - V_{\ell}(r) \hat{u}_{\ell}(r,\omega) e^{-i\omega t}\right] = 0$$

$$\left[\frac{\partial^{2} \hat{u}_{\ell}(r,\omega) e^{-i\omega t}}{\partial r_{*}^{2}} + \left(\omega^{2} e^{-i\omega t} \hat{u}_{\ell}(r,\omega)\right) - V_{\ell}(r) \hat{u}_{\ell}(r,\omega) e^{-i\omega t}\right] = 0$$
(A.1)

Equation (A.1) is referred as **Regge-Wheeler equation**.

Appendix B

Deriving equation (3.1)

The Schwarzschild metric is given by -

$$ds^{2} = -\left(1 - \frac{2GM}{r}\right)dt^{2} + \left(1 - \frac{2GM}{r}\right)^{-1}dr^{2} + r^{2}d\Omega^{2}$$
 (B.1)

Where $d\Omega^2 = d\theta^2 + \sin^2\theta d\phi^2$ (Angular part of metric). Now, for radially outgoing null geodesic, angular components $(d\theta, d\phi)$ vanishes, i.e. $(d\Omega^2 = 0)$. Therefore, the Schwarzschild metric for radial geodesic $(d\theta = d\phi = 0)$ is:

$$ds^{2} = -\left(1 - \frac{2GM}{r}\right)dt^{2} + \left(1 - \frac{2GM}{r}\right)^{-1}dr^{2}$$
 (B.2)

For null geodesic $(ds^2 = 0)$

$$0 = -\left(1 - \frac{2GM}{r}\right)dt^2 + \left(1 - \frac{2GM}{r}\right)^{-1}dr^2$$

$$\left(1 - \frac{2GM}{r}\right)dt^2 = \left(1 - \frac{2GM}{r}\right)^{-1}dr^2$$

$$dr^2 = \left(1 - \frac{2GM}{r}\right)^2dt^2$$

$$dr = \left(1 - \frac{2GM}{r}\right)dt$$
(B.3)

let's define Tortoise coordinate r_* as :

$$r_* = r + 2GM \ln \left(\frac{r}{2GM} - 1\right) \tag{B.4}$$

Differentiating both sides,

$$dr_* = dr + (2GM) \left(\frac{1}{\frac{r}{2GM} - 1}\right) \left(\frac{1}{2GM}\right) dr$$
$$dr_* = dr + \frac{dr}{\left(\frac{r}{2GM} - 1\right)}$$

$$dr_* = \left(1 + \frac{1}{\left(\frac{r}{2GM} - 1\right)}\right) dr$$

$$dr_* = \left(\frac{\frac{r}{2GM} - 1 + 1}{\frac{r}{2GM} - 1}\right) dr$$

$$dr_* = \left(\frac{\frac{r}{2GM}}{\frac{r}{2GM} - 1}\right) dr$$

$$\therefore dr = \left(\frac{\frac{r}{2GM} - 1}{\frac{r}{2GM}}\right) dr_*$$

$$dr = \left(1 - \frac{1}{\frac{r}{2GM}}\right) dr_*$$
(B.5)

Substituting (A.5) in (A.3) we get,

$$\left(1 - \frac{1}{\frac{r}{2GM}}\right)dr_* = \left(1 - \frac{2GM}{r}\right)dt$$

$$dr_* = dt$$

$$t = r_* + C \tag{B.6}$$

Let's define a small quantity u:

$$u = \frac{r}{2GM} - 1 \tag{B.7}$$

$$\therefore r = 2GM(1+u) \tag{B.8}$$

From (A.4) we have :

$$r_* \approx 2GM + \ln\left(\frac{r}{2GM} - 1\right)$$

$$r_* \approx 2GM + \ln\left(\frac{2GM(1+u) - 1}{2GM}\right)$$

$$\therefore r_* \approx 2GM \ln(u) \tag{B.9}$$

Substituting (A.9) in (A.6) we get,

$$t = 2GM\ln(u) + C$$

Now, from the logarithm identity we have:

$$\ln(u) = -\ln\left(\frac{1}{u}\right)$$

Thus,

$$t = 4GM \ln\left(\frac{1}{u}\right) + C + \mathcal{O}(u)$$

Appendix C

Deriving equation (3.2)

From equation (3.1) we have,

$$t = 4GM \log \left(\frac{1}{u}\right) + C$$

$$t - C = 4GM \log \left(\frac{1}{u}\right)$$

Now, from the property of Logarithm,

$$\log\left(\frac{1}{u}\right) = -\log u$$

Substituting this property in the above equation we get :

$$t-C=4GM\left(-\log\left(u\right)\right)$$

$$\frac{t - C}{-4GM} = \log\left(u\right)$$

Taking exponent on both sides,

$$e^{(t-C/-4GM)} = u$$

$$\therefore u = e^{(t/-4GM)} e^{(-C/-4GM)}$$

$$u = e^{(t/-4GM)} e^C$$

$$\therefore \left(e^{(-C/-4GM)} = e^C \right)$$

Thus,

$$u = e^C e^{(t/-4GM)}$$

Appendix D

Deriving equation (3.5)

From equation (3.2) we have,

$$u = e^C e^{-t/4GM}$$
 , $u' = e^C e^{-t'/4GM}$

$$du = e^{C} \left(-\frac{1}{4GM} \right) e^{-t/4GM} dt \quad , \quad du' = e^{C} \left(-\frac{1}{4GM} \right) e^{-t'/4GM} dt'$$

Substituting the above relations on equation (3.4) we get,

$$\langle \psi(t)\psi(t')\rangle = \frac{(dudu')^{1/2}}{u - u'}$$

$$= \frac{\left[(e^C \left(-\frac{1}{4GM} \right) e^{-t/4GM} dt) \times (e^C \left(-\frac{1}{4GM} \right) e^{-t'/4GM} dt') \right]^{1/2}}{e^C e^{-t/4GM} - e^C e^{-t'/4GM}}$$

$$= \frac{e^C \left(\frac{1}{4GM} \right) \left[e^{-t/4GM} dt \right) \times e^{-t'/4GM} dt')}{e^C (e^{-t/4GM} - e^{-t'/4GM})}$$

$$= \left(\frac{1}{4GM}\right) \frac{\left[e^{-t-t'/4GM}dtdt'\right]^{1/2}}{e^{-t/4GM} - e^{-t'/4GM}}$$

$$= \left(\frac{1}{4GM}\right) \frac{\left(e^{-t-t'/4GM}\right)^{1/2} \left(dtdt'\right)^{1/2}}{e^{-t/4GM} - e^{-t'/4GM}}$$

$$\therefore \langle \psi(t)\psi(t') \rangle = \left(\frac{1}{4GM}\right) \frac{e^{-t-t'/8GM} (dtdt')^{1/2}}{e^{-t/4GM} - e^{-t'/4GM}}$$
(D.1)

Simplifying the denominator,

$$e^{-t/4GM} - e^{-t'/4GM}$$

We can write,

$$e^{-t/4GM} = e^{-t/8GM} \times e^{-t/8GM}$$

Similarly,

$$e^{-t'/4GM} = e^{-t'/8GM} \times e^{-t'/8GM}$$

$$\therefore e^{-t/4GM} - e^{-t'/4GM} = \left(e^{-t/8GM} \times e^{-t/8GM}\right) - \left(e^{-t'/8GM} \times e^{-t'/8GM}\right)$$
$$e^{-t/4GM} - e^{-t'/4GM} = \left(e^{-t/8GM} \times e^{-t'/8GM}\right) \left(e^{(t-t')/8GM} - e^{-(t-t')/8GM}\right)$$
(D.2)

Substituting (C.2) in (C.1) we get,

$$\langle \psi(t)\psi(t')\rangle = \left(\frac{1}{4GM}\right) \frac{e^{-t-t'/8GM} (dtdt')^{1/2}}{\left(e^{-t-t'/8GM}\right) \left(e^{(t-t')/8GM} - e^{-(t-t')/8GM}\right)}$$

Thus,

$$\langle \psi(t)\psi(t')\rangle = \left(\frac{1}{4GM}\right) \frac{\left(dtdt'\right)^{1/2}}{\left(e^{(t-t')/8GM} - e^{-(t-t')/8GM}\right)}$$

Appendix E

To show equation (3.5) is Antiperiodic in imaginary time:

From equation (3.5) we have,

$$\langle \psi(t)\psi(t')\rangle = \left(\frac{1}{4GM}\right) \frac{(dtdt')^{1/2}}{(e^{(t-t')/8GM} - e^{-(t-t')/8GM})}$$

Substituting $t \to t + 8\pi GMi$ in the above equation :

$$\langle \psi(t + 8\pi GMi) \psi(t') \rangle = \left(\frac{1}{4GM}\right) \frac{(dtdt')^{1/2}}{(e^{(t+8\pi GMi-t')/8GM} - e^{-(t+8\pi GMi-t')/8GM})}$$

Simplifying the denominator,

$$e^{(t+8\pi GMi-t')/8GM} = e^{(t-t')/8GM} e^{i\pi}$$

$$e^{-(t+8\pi GMi-t')/8GM} = e^{-(t-t')/8GM} e^{-i\pi}$$

Now, from Euler's formula we have,

$$e^{i\theta} = \cos\theta + i\sin\theta$$
 , $e^{-i\theta} = \cos\theta - i\sin\theta$
 $\therefore e^{i\pi} = \cos(\pi) + i\sin(\pi) = \cos(\pi) = -1$
& $e^{-i\pi} = \cos(-\pi) + i\sin(-\pi) = \cos(-\pi) = -1$

$$\therefore e^{(t+8\pi GMi-t')/8GM} = (-1) e^{(t-t')/8GM}$$

Similarly,

$$e^{-(t+8\pi GMi-t')/8GM} = (-1) e^{-(t-t')/8GM}$$

Thus, the denominator becomes,

$$(-1) e^{(t-t')/8GM} - (-1) e^{-(t-t')/8GM}$$
$$- e^{(t-t')/8GM} + e^{-(t-t')/8GM}$$
$$- \left(e^{(t-t')/8GM} - e^{-(t-t')/8GM}\right)$$

Thus, the equation becomes,

$$\langle \psi(t + 8\pi GMi) \psi(t') \rangle = -\left(\frac{1}{4GM}\right) \frac{(dtdt')^{1/2}}{(e^{(t-t')/8GM} - e^{-(t-t')/8GM})}$$
$$\left[\langle \psi(t + 8\pi GMi) \psi(t') \rangle = -\langle \psi(t) \psi(t') \rangle\right]$$

Thus, this property means the function is Antiperiodic with a period of $8\pi GMi$ in Imaginary time.

Appendix F

Wronskian of λ_{ω} and $\tilde{\lambda}_{\omega}$

At $r_* \to -\infty$:

$$W_{1} = \begin{vmatrix} e^{i\omega r_{*}} + R(\omega) e^{-i\omega r_{*}} & \widetilde{T}(\omega) e^{-i\omega r_{*}} \\ i\omega e^{i\omega r_{*}} - i\omega R(\omega) e^{-i\omega r_{*}} & -i\omega \widetilde{T}(\omega) e^{-i\omega r_{*}} \end{vmatrix}$$

$$= \left(-i\omega \widetilde{T}(\omega) e^{-i\omega r_{*}} \right) \times \left(e^{i\omega r_{*}} + R(\omega) e^{-i\omega r_{*}} \right) - \left(\widetilde{T}(\omega) e^{-i\omega r_{*}} \right) \times \left(i\omega e^{i\omega r_{*}} - i\omega R(\omega) e^{-i\omega r_{*}} \right)$$

$$= \left(-i\omega \widetilde{T}(\omega) \right) - \left(-i\omega \widetilde{T}(\omega) \right)$$

$$\therefore W_{1} = -2i\omega \widetilde{T}(\omega)$$
(F.1)

At $r_* \to \infty$:

$$W_{2} = \begin{vmatrix} T(\omega) e^{i\omega r_{*}} & e^{-i\omega r_{*}} + \widetilde{R}(\omega) e^{i\omega r_{*}} \\ i\omega T(\omega) e^{-i\omega r_{*}} & -i\omega e^{-i\omega r_{*}} + i\omega \widetilde{R}(\omega) e^{-i\omega r_{*}} \end{vmatrix}$$

$$= (T(\omega) e^{-i\omega r_{*}}) \times \left(-i\omega e^{-i\omega r_{*}} + i\omega \widetilde{R}(\omega) e^{i\omega r_{*}} \right) - \left(i\omega T(\omega) e^{i\omega r_{*}} \right) \times \left(e^{-i\omega r_{*}} + \widetilde{R}(\omega) e^{i\omega r_{*}} \right)$$

$$= \left(-i\omega \widetilde{T}(\omega) \right) - \left(-i\omega \widetilde{T}(\omega) \right)$$

$$\therefore W_{2} = -2i\omega \widetilde{T}(\omega)$$
(F.2)

From (E.1) and (E.2),

$$T(\omega) = \widetilde{T}(\omega)$$

Bibliography

- [1] Edward Witten. Introduction to Black Hole Thermodynamics. arXiv preprint arXiv:2412.16795, version 3, 2025. https://doi.org/10.48550/arXiv.2412.16795.
- [2] V. P. Frolov and I. D. Novikov, doi:10.1007/978-94-011-5139-9
- [3] T. Lancaster and S. J. Blundell, Oxford University Press, 2014, ISBN 978-0-19-969933-9
- [4] Unpublished Notes on Hawking Radiation by Mritunjay Kumar Verma.